

**DEVELOPMENT OF AN ITERATIVE  
LEARNING CONTROLLER FOR POLYMER  
BASED MICRO-STEREOLITHOGRAPHY  
PROTOTYPING SYSTEMS**

A THESIS SUBMITTED TO  
THE GRADUATE SCHOOL OF ENGINEERING AND SCIENCE  
OF BILKENT UNIVERSITY  
IN PARTIAL FULFILLMENT OF THE REQUIREMENTS FOR  
THE DEGREE OF  
MASTER OF SCIENCE  
IN  
MECHANICAL ENGINEERING

By  
Erkan Buğra Türeyen

August 2016

DEVELOPMENT OF AN ITERATIVE LEARNING CONTROLLER  
FOR POLYMER BASED MICRO-STEREOLITHOGRAPHY PRO-  
TOTYPING SYSTEMS

By Erkan Buğra Türeyen

August 2016

We certify that we have read this thesis and that in our opinion it is fully adequate,  
in scope and in quality, as a thesis for the degree of Master of Science.

---

Melih Çakmakcı (Advisor)

---

Yiğit Karpat

---

Kutluk Bilge Arıkan

Approved for the Graduate School of Engineering and Science:

---

Levent Onural  
Director of the Graduate School

## ABSTRACT

# DEVELOPMENT OF AN ITERATIVE LEARNING CONTROLLER FOR POLYMER BASED MICRO-STEREOLITHOGRAPHY PROTOTYPING SYSTEMS

Erkan Buğra Türeyen

M.S. in Mechanical Engineering

Advisor: Melih Çakmakkı

August 2016

Additive manufacturing systems provide fast and accurate fabrication opportunities for micro-scaled structures. Various methods of processing are used for fabrication of different materials. Stereolithography is an important technique for rapid prototyping of photo-reactive polymer based materials. Similar to the other additive manufacturing methods, DLP based projection micro-stereolithography also includes limitations in terms of dimensions, minimum feature sizes and material properties. For advanced and precise micro-sized structure fabrications, process needs to be defined with a complex control scheme.

In order to develop a scheme for increasing the fabrication quality, nature of the complex chemical and physical phenomena behind the resin solidification process is investigated. A complete mathematical model for the pixel based photopolymerization process is developed. According to the parameters included in the solidification model, measurements and observations are made for understanding of the resin, optical system and positioning system.

Problems of over-curing and under-curing caused by the attenuation nature of the light inside the liquid resin are observed in the simulations made based on the model which is also supported by the previous fabrication experiences for varying structures. These problems creating structural irregularities are dependent on the process parameter of exposure applied on the fabrication surface.

An iterative learning based parameter control algorithm is developed for overcoming these errors decreasing the fabrication quality. Continuous fabrication platform movement instead of step-by-step movement which is one of the main

features of the established system is used to define a solution. Main fabrication parameter of platform speed is adjusted for each layer according to the error amount calculated on iterations.

Use of an optimized gain for parameter control, decreased the dimensional error calculated by the count of the wrongly cured pixels up to 80% in the simulations and 75% in the real life fabrication trials with the application of algorithm. These improvement ratios and proposed algorithm provide a new perspective for the possible future work about online exposure measurement and in-situ parameter control of the stereolithography process.

*Keywords:* Additive Manufacturing, Micro Stereolithography, Iterative Learning Control, Over and Under Exposure, Pixel Cure Model.

## ÖZET

# POLİMER BAZLI MİKRO-STEREOLİTOGRAFI SİSTEMLERİ İÇİN YİNELEMELİ ÖĞRENME DENETİMİ ALGORİTMASI GELİŞTİRİLMESİ

Erkan Buğra Türeyen

Makine Mühendisliği, Yüksek Lisans

Tez Danışmanı: Melih Çakmakçı

Ağustos 2016

Eklemeli üretim sistemleri, mikro boyutlu yapıların üretilmesi için hızlı ve hassas çözümler sunmaktadır. Değişik malzemelerin üretilebilmesi için farklı metotlar kullanılmaktadır. Stereo-litografi, ışığa duyarlı polimer temelli malzemelerin hızlı modellenmesi için önemli bir yöntemdir. Diğer eklemeli üretim teknikleri gibi, DLP yansıtım ile mikro-stereo-litografi yöntemi de ölçüler, minimum detay boyutu ve malzeme özellikleri gibi alanlarda üretim limitlerine sahiptir. Gelişmiş ve hassas mikro boyutlu parçaların üretimi için, işlemin karmaşık bir kontrol algoritması ile tanımlanarak yönetilmesi ihtiyacı ortaya çıkmıştır.

Üretim kalitesinin arttırılması amacıyla bir işlem planı hazırlanması, reçine katılaştırma işleminin arkasındaki karmaşık kimyasal ve fiziksel süreçlerin iyi araştırılmasıyla mümkün olacaktır. Bu sebeple, piksel temelli polimerizasyon işleminin matematik modeli oluşturulmuştur. Katılma modeli içerisinde bulunan parametrelerden yola çıkılarak; reçine, optik sistem ve pozisyonlama sistemleri üzerinde farklı ölçümler ve gözlemler gerçekleştirilmiştir.

Modelin kullanımı ile yapılan benzetimlerde, ışığın sıvı reçine içerisindeki güçsüzleşmesinden kaynaklanan ve önceden yapılan üretim denemelerinde de gözlemlenmiş olan aşırı katılma ve yetersiz katılma problemleri ile karşılaşmıştır. Yapısal bozulmalara sebep olan bu hataların, üretim yüzeyine uygulanan ışık miktarını belirleyen maruz kalma parametresine bağlı olduğu belirlenmiştir.

Üretim kalitesini düşüren bu hatanın bertaraf edilmesi amacıyla yinelemeli öğrenme temelli parametre kontrol algoritması geliştirilmiştir. Kullanılan üretim

sisteminin ana özelliklerinden olan adım adım hareket yerine üretim platformunun sürekli hareketinin sağlanması, çözüm oluşturulmasında ana kaynak olarak kullanılmıştır.

Optimize edilmiş bir kazanım değerinin parametre kontrolü amacıyla kullanılması ile, yanlış katılaştırılan piksellerin oranı simülasyonlarda %80'e, gerçek üretim denemelerinde ise %75'e varan oranlarda azaltılmıştır. Bu gelişme oranları ve bahsedilen algoritma, gelecekte eş zamanlı ışık gösterimi ölçümünün ve eş zamanlı stereo-litografi işlemi kontrolünün oluşturulması için yeni bir perspektif oluşturacaktır.

*Anahtar sözcükler:* Eklemeli Üretim, Mikro-Stereolitografi, Yinelemeli Öğrenme Denetimi, Aşırı ve Yetersiz Işık Gösterimi, Piksel Katılma Modeli.

## Acknowledgement

Firstly, I would like to express my deep gratitude to my academic advisor Prof. Melih Çakmakçı, who gave me an incredible amount of support during my degree research with his high level of understanding, devotion and goodwill. The most common and reasonable expectations of a graduate student are all hidden within his very own character, mentality and enthusiasm. All the great experience like conferences we have attended and successful improvements we have achieved throughout my research, depends on his belief on my working ambition and our impressive and entertaining research subject, additive manufacturing. It is also a genuine pleasure to express my deep sense of thanks and gratitude for the common work on our project collaborator Prof. Yiğit Karpaz and his student, my research partner Zulfiqar Ali.

I am hugely indebted and grateful to my parents Gülşen and Suat Türezen for their trusting and loving support, but more than anyone to my beautiful and smart sister Esra. I should not forget to thank with all my heart to my closest relatives, uncles, my lovely aunt and most importantly my dear and beloved grandparents. Furthermore, life in Ankara and life in the university is nothing but your friends with their presence and backing on every step of all the hard and good times. I should thank to Serhat, Mümtaz, Atakan and Alper for the unforgettable times hopefully eternal friendship during my masters. Starting from the undergraduate school, Sinan, Dilşad, Alp, Ersun, Arda and other members of our great team gave me their warm-hearted companionship on everything about life and I am extremely thankful for their valuable existence. Last but not least, my dear love and endless best friend Yasemin has always been one of my greatest supporter and cheerful partner on every single day that we have been together. I have an infinite gratitude and happiness for her precious existence in my life.

This research is sponsored by Scientific and Technical Research Council of Turkey (TUBITAK), Project No: 113M172. [‘Development of an Multipurpose Micro Manufacturing System using Modular and Iterative Learning Control Algorithms’]

# Contents

- 1 Introduction** **1**
- 1.1 Stereolithography . . . . . 1
- 1.2 Micro Stereolithography . . . . . 3
- 1.3 System . . . . . 6
  - 1.3.1 Working Scheme . . . . . 6
  - 1.3.2 Components . . . . . 8
  - 1.3.3 Applications . . . . . 9
  - 1.3.4 Measurements . . . . . 11
- 1.4 Projection Lithography Control . . . . . 12
- 1.5 Motivation and Contributions . . . . . 15
  
- 2 Mathematical Modeling** **18**
- 2.1 Layer Cure Model . . . . . 19
- 2.2 Process Parameter . . . . . 26

2.3 Pixel Cure Model . . . . . 27

**3 Development and Validation of the Control Algorithm 30**

3.1 Iterative Learning Control Algorithm . . . . . 30

3.1.1 Single Layer Based . . . . . 30

3.1.2 Advanced Multiple Layer Based . . . . . 37

3.2 Simulations . . . . . 38

3.2.1 Basic Shape . . . . . 38

3.2.2 Complex Shape . . . . . 42

3.3 Validation of the Algorithm . . . . . 43

3.3.1 Experimental Design . . . . . 44

3.3.2 Basic Shape . . . . . 45

3.3.3 Complex Shape . . . . . 46

3.3.4 Analysis of Results . . . . . 55

**4 Conclusion and Future Work 60**

**Bibliography 64**

**A Matlab Code 68**

A.1 Image Processing . . . . . 68

A.2 Actual Model Simulation . . . . . 69

A.3 Reference Model Simulation . . . . . 70

A.4 Error Calculation . . . . . 70

A.5 3D Simulation Result . . . . . 71

A.6 Parameter Control Algorithm . . . . . 71

**B Nomenclature 73**

# List of Figures

1.1	One of the first fabrication trials using laser stereolithography for accurate shape solidification. [12] . . . . .	4
1.2	Sun [13] uses a digital micro-mirror device and a projection lens in his micro-stereolithography setup. . . . .	5
1.3	Highly precise parts with tunable mechanical properties fabricated by the laser based stereolithography system developed by Stampfl. [17] . . . . .	6
1.4	DLP stereolithography system. . . . .	7
1.5	Developed systems working scheme. . . . .	7
1.6	Fabricated high aspect ratio structures. . . . .	9
1.7	Measurements of fabricated micro needle structures. . . . .	10
1.8	Fabricated parts including varying materials with different properties. . . . .	11
1.9	Microscopes used as the main measurement devices. . . . .	12
1.10	Decrease in the formation of stair like structures with grey-scale image projection technique developed by Pan. [27] . . . . .	14

1.11	Layer by layer fabrication with the use of 25 $\mu m$ layer height and result of continuous fabrication platform motion usage. [28] . . . .	15
1.12	Over cured areas at the bottom and under cured areas at the top side of the structure . . . . .	17
2.1	Power meter setup to find the irradiation of DLP projector. . . .	21
2.2	Pixel intensity values of a specific area. . . . .	22
2.3	Result of FTIR testing, showing the percent of transmittance for different wavelengths. . . . .	23
2.4	Results of experiment with platform at distance of 5mm and exposure time from 45 to 180 seconds. . . . .	25
2.5	Intensity difference between the reference and actual irradiations.	28
3.1	Expected versus real life energy distribution on surface. . . . .	32
3.2	Example mesh data on x-y-z layers for simulation of over-cure and under-cure errors. . . . .	33
3.3	$\mu$ SLA System block diagram. . . . .	35
3.4	Diagram of iterative learning scheme and fabrication process. . .	36
3.5	Reference layer image and projected layer image. . . . .	39
3.6	Reference and simulated structures created with the process simulation algorithm. . . . .	40
3.7	Layer number vs exposure time graph. . . . .	40
3.8	Layer number vs error graph. . . . .	41

3.9	Expected vs actual layer projections on the surface for complex structure. . . . .	42
3.10	Simulated fabrications for complex shape. . . . .	43
3.11	Initial fabrication of the simple shape design with the desired CAD model. . . . .	45
3.12	Fabrication results of the basic shape with and without using the algorithm. . . . .	47
3.13	Measurement on the right side shows without the algorithm the depth of the hole is 1mm but using the algorithm depth reaches 6 <i>mm</i> . . . . .	49
3.14	Over-cured areas disappear by using the algorithm (a), fabrication example with the starting parameter of the algorithm (b). . . . .	49
3.15	Fabrication trials with fixed exposure times of 4, 3 and 2 seconds and fabrication times of 40, 30 and 20 mins. . . . .	50
3.16	Fabrication of the complex shape using adjusted parameters found with the use of iterative learning scheme in a total fabrication time of 15 mins. . . . .	51
3.17	Design of the gear structure with actual and reference images. . .	52
3.18	Picture a shows the fabrication without algorithm. Picture b, c and d is results of fabrications with the algorithm but changing amount of gains. . . . .	52
3.19	Fabrication without and with the use of the algorithm on scale x2.5.	53
3.20	Fabrications with scale x2. . . . .	53
3.21	Fabrications with different dimensional scales. . . . .	54

3.22	Image showing the high amount of over-curing under the stair shape.	57
3.23	Upside-down and straight positioned fabrications of stair like structures without the algorithm. . . . .	58

# List of Tables

2.1	Results of critical irradiation experiment . . . . .	26
3.1	Differences between varying single layer fabrication times . . . . .	52
3.2	Measured vs. actual dimensions in different scaled gear fabrications.	54

# Chapter 1

## Introduction

### 1.1 Stereolithography

Additive manufacturing is recently an important and greatly developing technology for fast and accurate fabrication of 3 dimensional objects. Also called as the rapid prototyping, this technology is a huge advancement for precision manufacturing, mainly for prototyping practices and lately for mass production of various structures with the use of different materials. This technology includes lots of different techniques for fabrication, mainly differing from the point of used materials and desired final product properties.

An example of these techniques is selective laser sintering for fabrication of aluminum alloy powdered structures in different industries like automotive, aerospace and even for dental applications. Sintering provides high quality and low cost fabrications when compared to classical manufacturing methods. This technique is composed of complex chemical and physical processes based on the metallurgical bonding of powder layers. Also lots of different scientific research areas are included like chemistry, metallurgy, optics, heat transfer, etc. [1]

Another example of additive manufacturing methods is the layer by layer fabrication of polymer based materials and hybrid compounds with a technique called stereolithography. This technique is based on solidification of liquid materials with a light source. Chosen light source could be a laser or a DLP projector that can provide the necessary irradiation on the resin. This process involves separate sub-systems for increasing the productivity. Apart from the light source, a positioning system and an optical device array is also integrated into these systems.

Light source is used to provide the energy that will be applied on the resin for creating the polymerization process. As an example Zhang [2] uses a femto-second laser for photo-polymerization with nano-imprinting for direct digital manufacturing. This nano fabrication process is used to create nano-molds for further fabrication purposes. DLP (direct light processing) devices are also used instead of the lasers for lithography based additive manufacturing. Hatzenbichler [3] uses direct light projection technology for layer by layer manufacturing of ceramic parts using ceramic-filled photosensitive resins. For fabrication of desired surfaces and precise generation of 3 dimensional structures out of single layers is mostly used with the help of a mask structure. Choi [4] uses a dynamic mask projection system in his test setup for controlling the cure depth for fabricating complex 3d micro-structures. A digital micro-mirror device (DMD) is used for high resolution masking of the light source while being projected on the fabrication area. Hatzenbichler [5] uses Texas Instruments DLP Lightcrafter as the light source for providing irradiation on the fabrication area. Research results showed good fabrications of  $250 \mu m$  wall thickness.

Optics is another important aspect of the stereolithography process. When a laser is used in the system as the light source, waves coming out could be directed to the fabrication surface with lenses and a tunable mirror like the setup used by Lee [6]. When a projector is used as the light source, Chiu [7] uses a set of optical lenses for rescaling the projected image and also for providing the best resolution possible to the light rays coming out of the DLP projector, which is also used as a masking device.

This fabrication technique is used in lots of different areas for manufacturing of various structures. Berger [8] uses stereolithography for fabrication of high reduction polymer gears. He found out that the gears can be manufactured for lower costs, with decreased manufacturing times and even the miniaturization of gear sizes is easily applicable. Au [9] uses stereolithography for fabrication of micro-fluidic devices even though classical lithography and other clean room fabrication techniques are mostly used to fabricate these types of devices. Au, revealed that stereolithography provides a more efficient fabrication of 3d structures in terms of cost, speed and convenience and also not producible through methods like PDMS molding.

Medical sector and tissue based researches are also widely related with the additive manufacturing and stereolithography. Complex porous tissue engineering scaffolds are fabricated by Gauvin [10]. These scaffolds are used for supporting the cell growth in accurately manufactured 3d structures. Meyer [11] uses stereolithography technique for fabrication of small blood supplying systems. Their research includes measuring of material properties like tensile strength, definition of bio-compatibility according to chemical structure and investigation of photo-polymerization. Also processing parameters of stereolithography in terms of curing speeds is evaluated.

## 1.2 Micro Stereolithography

Stereolithography for fabrication of micro-sized parts and structures is an important topic of research. This topic also originates the main aim for this thesis. Fabrications of high precision structures are used in many different applications like micro sensors, micro medical devices and moving multi piece mechanisms. One of the preliminary researches of Partanen [12] was describing a laser based stereolithography system with 100 micron resolution for fabrication of connector pin structures with 300  $\mu m$  pitch. (*Fig. 1.1*)

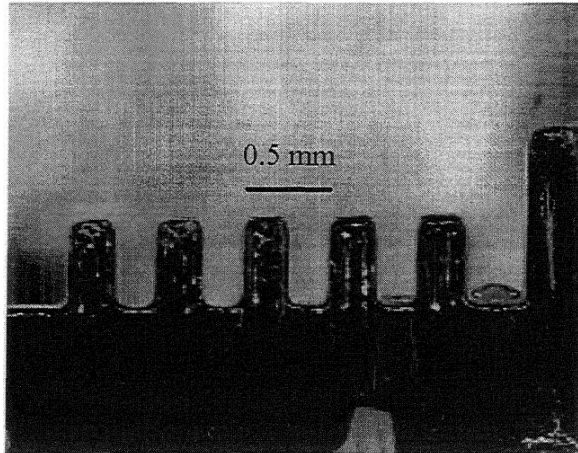


Figure 1.1: One of the first fabrication trials using laser stereolithography for accurate shape solidification. [12]

Sun [13] uses the DMD device as a dynamic mask for fabrication of complex structures with micro-stereolithography. Dynamic masking provides high resolution projection on the fabrication surface. Also a projection lens is included in this system for adjusting the dimensions of the masked image to the fabrication platform placed on a positioning system called as the elevator. (*Fig. 1.2*)

Various material usages are valuable as stereolithography systems are limited with photo reactive substances. Hadipoespito [14] proposes micro fabrication of transparent polymers and nano-composites with stereolithography technique. Especially micro gear shapes are fabricated in his research with  $20 \mu m$  resolution.

Ovsianikov [15] investigated micro-fabrication of 3 dimensional scaffolds for tissue engineering. Using two-photon polymerization technique, structures down to  $7 \mu m$  width can be fabricated. This is a different technique in which a specialized lase is used in a complex system. These hugely precise fabrications are also proven to be effective for even  $100 nm$  structural resolution.

Lee [16] makes an investigation of similarly precise manufacturing objectives based on LCD micro-stereolithography. Making calculations for finding the relationship between the cure depth amount and exposure was used for observing the solidification characteristics. Ceramic reinforced resin is used for fabrication of bevel gears with  $400 \mu m$  center diameter. Layer thickness down to  $10 \mu m$

is reached with the use of an efficient technique called greyscale masking. This technique is based on use of grey scaled projected layer images instead of black and white images used in classical stereolithography.

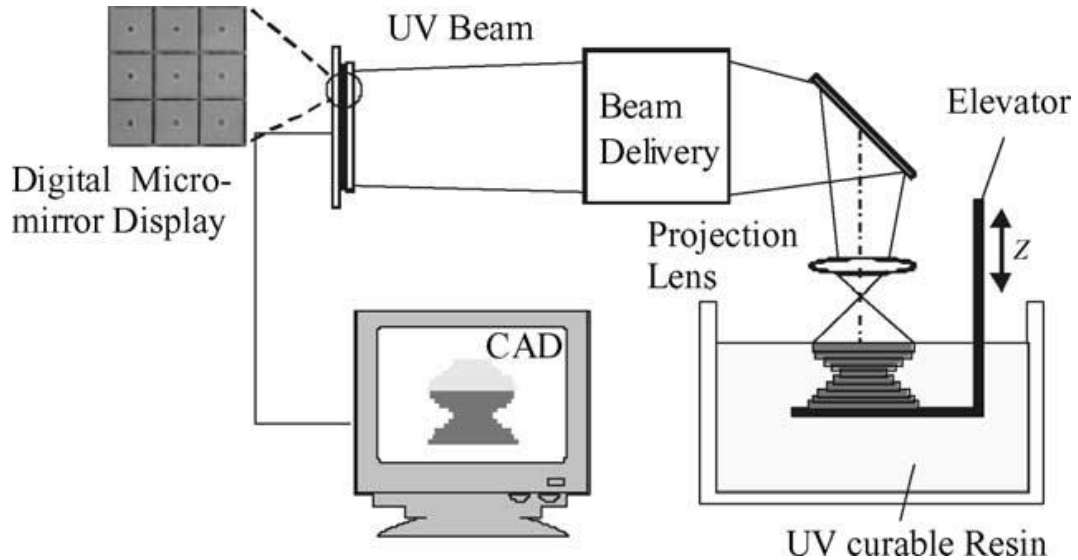


Figure 1.2: Sun [13] uses a digital micro-mirror device and a projection lens in his micro-stereolithography setup.

Material properties are a vastly important subject of additive manufacturing. Formation of previously defined material characteristics during the fabrication is a desired aspect especially for manufacturing of micro structures. Stampfl [17] proposes a system working based on a laser light source that can fabricate parts with tunable material properties. Use of different photo-reactive resins made it possible to fabricate movable parts, elastomeric behaving parts and micro-channels with high aspect ratios up to 30. (*Fig. 1.3*)

Micron level accurate structures are difficult to fabricate in terms of positioning and small exposure image formation. But also main logic of stereolithography process based on layer-by-layer fabrication of structures creates a challenge according to the number of layers generated. Because of the layered parts manufactured, deficiencies are observed in the inter-layer areas. Nature of polymerization results in stair like structures at these layer joint areas.

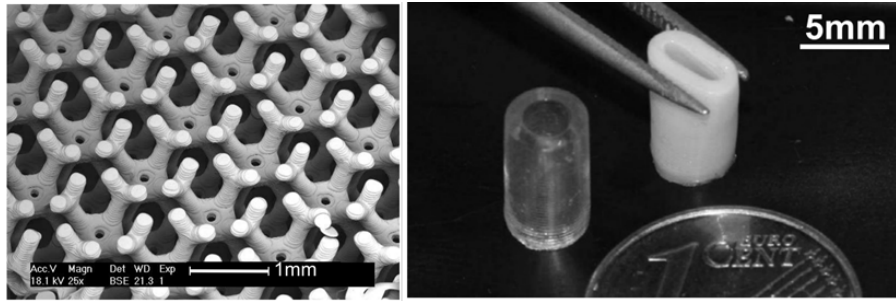


Figure 1.3: Highly precise parts with tunable mechanical properties fabricated by the laser based stereolithography system developed by Stampfl. [17]

## 1.3 System

Established and used system in this thesis is described in detail under this section. For clear understanding of the process and setup in detail, main working scheme, components included, parameters controlling the system and possible applications of the device are described separately.

### 1.3.1 Working Scheme

DLP based stereolithography system developed during this research is shown in Figure 1.4. A red colored protection box is used to block the outer lights in a certain wavelength interval from entering the fabrication area. Established system has an experimentally proved 25 microns resolution that is reached during the fabrication trials.

Main working scheme of the stereolithography process is defined in the previous chapters. In contrary with most of the more complex systems using lasers as the UV light source for the fabrication process, established system in this research uses a DLP projector as the light source and direct layer image projection device in the process. (*Fig. 1.5*) Young Optics DLP Lightcrafter is the used projector in the system because of its long usage interval, small size, lightness and easily controllable light intensity. System is established with an effective positioning system capable of high precision movement.

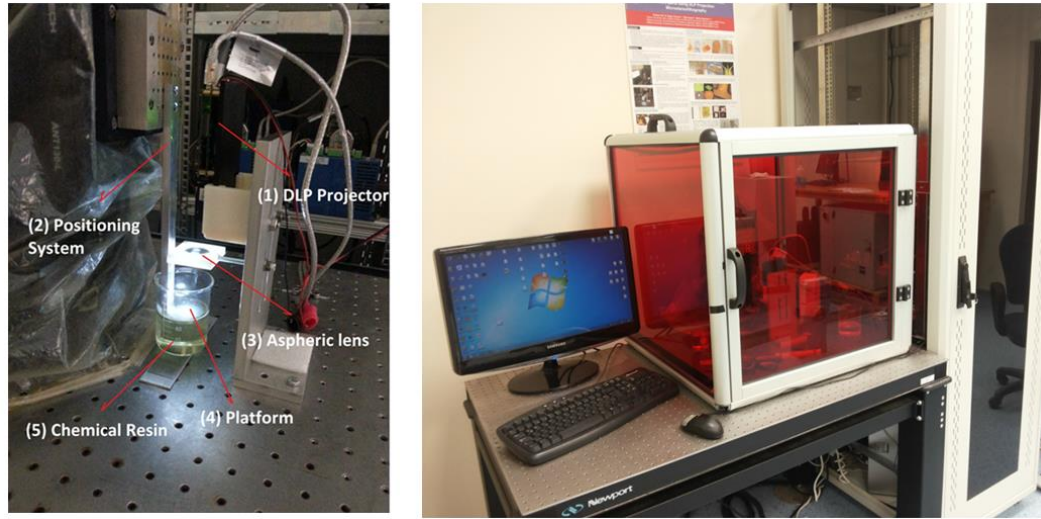


Figure 1.4: DLP stereolithography system.

Again diversified from the classical stereolithography systems, fabrication platform moving inside the resin container makes a continuous motion instead of step by step motion. This gradual movement of the platform or another part of the system is common in nearly all of the other additive manufacturing techniques as layer by layer solidification is the intention. This change is made with the goal of decreasing the fabrication errors and reaching flat surfaces with no signs on layer contact areas.

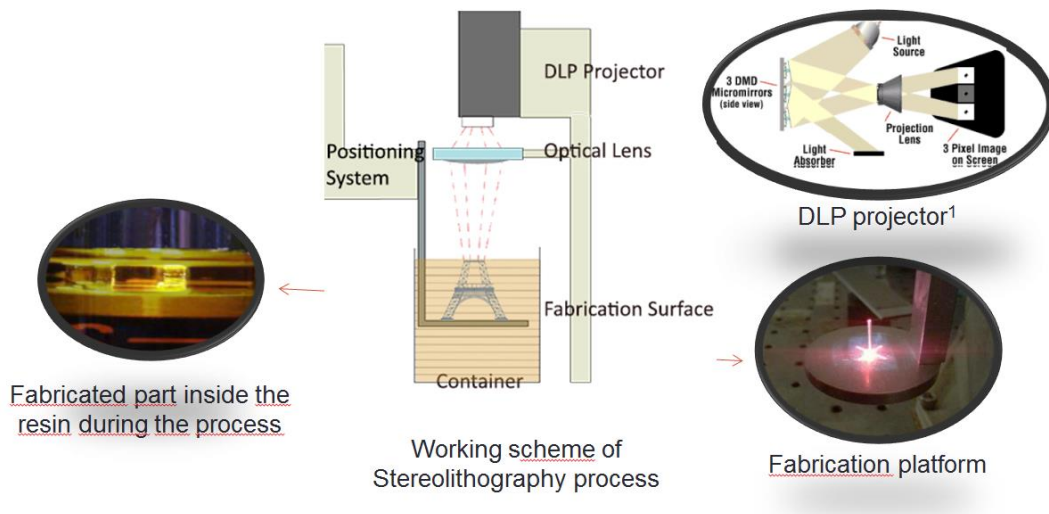


Figure 1.5: Developed systems working scheme.

### 1.3.2 Components

Optical System: Optical component which is placed between the DLP projector and fabrication surface converges the light rays that are projected in a diverging manner. Fabrication quality and reaching the minimum possible detail sizes with the used system is an important aspect mainly provided by the optical sub-system of the established device. With use of an achromatic and aspheric optical lens with 25 *mm* diameter and 50 *mm* focus length, chromatic and light ray transmission aberrations are kept in the minimum level which could potentially affect the quality of light transmitted through the projector to the fabrication surface. The optical lens is procured from the Newport Optics. These properties increased the quality of the layer image reflected on the surface. Also coating on the optical lens selectively eliminates the light rays which are located in a higher or lower level when compared to a specific interval close to UV region in wavelength scale. 400-700 *nm* wavelength regime is the provided interval for the optimization of color and spherical aberrations.

Positioning System: For precise movement and positioning of the fabrication platform, a 3-axis positioning system composed of Aerotech ultra-precision linear motor stages is used. These devices provide a 1nm minimum incremental motion with 40nm unidirectional repeatability. Only the z-axis stage providing the continuous motion of the fabrication platform is used for the stereolithography process. But it is also possible to use the motion of other axis for development of complex control system for the manufacturing processes.

Resin: Material is the most important aspect in additive manufacturing applications as they define the fabricated parts characteristics and usage areas. Polymer photo-active resin used is prepared in house within the context of the research. Rates of 3 different chemical substances used in the mixture of the resin is carefully measured and included.

Sudan 1 material is the UV absorber included in the mixture with an amount of 0.015g. Second material Phenylbis phosphine oxide is the photo initiator which ensures the linkage of bond and creation of polymer chains. Amount of the

material is 2 grams for a single bottle of resin. Third material which is the polymer itself named as the polyethylene glycol diacrylate. The amount of polymer in the mixture is 98ml. These 3 materials are left in a magnetic mixer for 3 days for homogenous creation of the resin.

Phenomenon of solidification starts with the application of the UV light to the resin. As the absorber increases the rate of UV emission, initiator material becomes reactive with the liquid monomer. This reaction starts the creation of polymer bonds as strong covalent bonds are formed between the cross links and polymer chains. Polymerization process defining this chemical reaction is the creation of large molecules called polymers from the congregation of small molecules names as monomers.

### 1.3.3 Applications

High Aspect Ratio Polymer Structures: One of the very first fabrication trials with the established system was made with high aspect ratio structures which is an important subject on manufacturing.(*Fig. 1.6*) Apart from the methods like injection molding, use of additive manufacturing techniques for fabrication of high aspect ratio structures offers distinct advantages. Experimental methods are used to define optimized process parameters and increase the fabrication quality. Influence of the light intensity and positioning system on the part quality is investigated. According to design of experiment, various tests and analysis have been performed to see the conformity of the fabricated parts to the original cad design. Optimization resulted on decrease of the error amounts more than 90%.

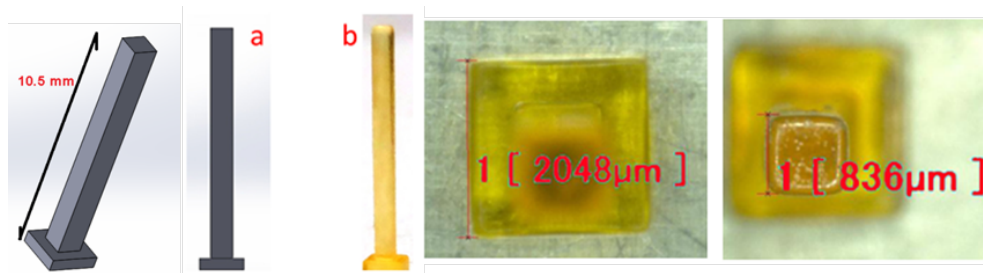


Figure 1.6: Fabricated high aspect ratio structures.

Polymer Micro Needles: Polymer micro-needles are widely researched devices because of the increased amount of usage in the medical industry. It is possible to manufacture them with various techniques. One of these techniques is the additive manufacturing and micro- stereolithography. Therefore trials to fabricate micro needle structures are done and  $40 \mu m$  tip diameter needles can be produced.(*Fig. 1.7*) These structures were important to test the limits of system in real life application for fabrication of the high aspect ratio structures and micron sized needles placed inside batches of tens of them.

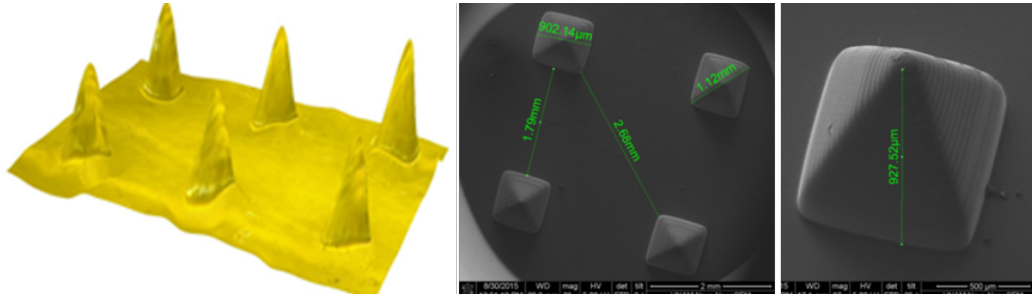


Figure 1.7: Measurements of fabricated micro needle structures.

Micro Sensors: Various manufacturing trials are done with the established system for the production of micro sensor parts and housings.(*Fig. 1.8*) These production examples are mainly based on using additive manufacturing for covering the outer area of electrical components like piezoelectric sensors. Initial trials was designed to test the capability of the system for adding piezoelectric like lead pieces during the 3d printing process, manually with the use of a holder. These trials succeeded as lead pieces were placed correctly without creating defects on the already manufactured layers and also process continued without delays or manufacturing errors.

Secondary trials are done to observe if it is possible to make additive manufacturing on the outer side of a piezoelectric material placed on the manufacturing platform using the commercial hard resin. Reason of hard resin usage is providing protection to the electrodes of the piezoelectric material and increase the durability of the electrode connections. For these productions, firstly the piezoelectric parts are placed on a previously printed surface. These surfaces are fixed

on the production platform. Then the platform is dipped inside the resin for the start of the process and curing of the initial layer. At the end of the productions, fully functioning piezoelectric sensors with electrodes hidden inside the 3d printed material are manufactured.

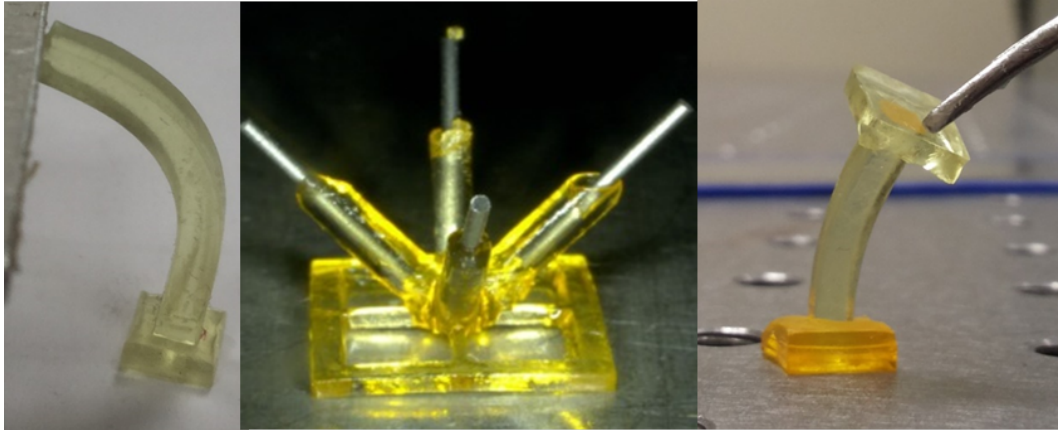


Figure 1.8: Fabricated parts including varying materials with different properties.

Also fabrications to combine materials with different properties on a single structure are made.(*Fig. 1.8*) Apart from the basic resin that has been used in all research trials, fabrications with hard and elastic commercial resins are used. These 3 different materials are combined on a single structure for being the base of further research about the development of micro sensors with materials having multiple properties on different sections.

### 1.3.4 Measurements

Measurement on this thesis and research is done with 2 different microscopes. Keyence branded VHK digital microscope and VKX 3D laser scanning confocal microscopes are used in detailed monitoring of the fabricated products.(*Fig. 1.9*) Dimensions like width, length, height and volumes are calculated with both of the devices. Complex examinations of the parts based on their volumes, 3D scanning of the shapes and depth measurements are also applied especially using digital microscope.



Figure 1.9: Microscopes used as the main measurement devices.

## 1.4 Projection Lithography Control

Additive manufacturing systems use various types of control algorithms for creating efficient and precise fabrication processes. Yebi [18] works on exposure time control on radiation based curing, for fabrication of layers to create thick structures. Firstly, a mathematical expression of the curing process including the solidification kinetics and heat radiation inside the material is developed. Based on the modeling, inter-layer holding time and layer exposing time of step by step fabrication process is optimized. This research is important based on the understanding of the solidification as similarly to the aim of the thesis, a control scheme is developed by Yebi using the process model.

Many process control methods are developed in order to improve the cured part features. Jariwala [19] worked on thin film fabrication using the projection micro-stereolithography method. Mathematical modeling of the curing process based on the previously defined main process parameters is generated. Using the model and precise movement of the DMD mirrors controlling the irradiated pixel areas, exposure time is aimed to be minimized and bitmap image formation which can also be called as DMD based masking is directed. Solidification model dependent control of the image masking and exposure timing is proven to be an effective way of process improvement. This control also provided dimensional error amounts to be kept less than 5%.

Zhao [20] worked on the process plan generation for decreasing the layer-by-layer fabrication based stepping errors in his thesis work. Complex modeling of the process using the feedback of measured topology is used to optimize the parameters. Optics, polymer solidification chemistry and mask image based geometrical structure formation is defined separately before generating the whole process model. Also effect of bitmap amounts are investigated as an important aspect on stepped layer formation for stereolithography process.

Yebi [21] proposes a partial differential equation based resin solidification process control. Apart from the other papers of Yebi for process modeling, curing is defined with a differential equation. Using the heat transfer model, for reaching the optimal fabrication area heat variation, irradiation input is adjusted with feedback control. Model uses the attenuation nature of light inside the photo reactive resin, for heat transfer trajectory assumption. Using this calculation and process error estimation, algorithm also utilizes a feed-forward scheme that is aimed to improve the feedback acquisition.

Control of the projection lithography process is an important research topic especially taking the online process observation techniques into consideration. Zhao [22] proposes two different techniques for both exposure time and applied light intensity control for the UV projection lithography. One is named as Evolutionary Cycle to Cycle and the other is Adaptive Neural Network Back-stepping. These controlling schemes both provide in-situ control and variable prediction calculations. Proposed algorithms are shown to be suitable for immediate adjustment of intensity and exposure during the solidification.

Jariwala [23] used Interferometric Curing Monitoring system developed by Jariwala [24] for observation of small regional solidifications in the resin. Adjusting of highly precise laser beam positioning provided measurement of polymerization. This real-time monitoring scheme of the stereolithography process is an important guide way for further online process control algorithm development.

Yebi [25] developed a process observation scheme based on online measurement of the curing state. Live measurement of the process is an important aspect for

resin solidification parameter control as well as all additive manufacturing controlling schemes. Surface temperature variation during the process is measured online. Using their model of heat transfer and distribution on the surface, developed estimation model could make precise assumptions for the curing amount achieved.

This type of an observation scheme is important for further usage in online parameter adjustment according to the fabrications course. Potgieter [26] defined the effects of varying irradiance distributions on the fabrication surface. This variation of the light reflected on the surface is defined as one of the causes for the deficiencies observed on the fabricated parts.

Parameter control methods are mostly used for development of control schemes improving the process output properties. Other than these, couples of methods are proposed to increase the fabrication quality of the stereolithography process. Pan [27] used a method called grey-scale image formation for overcoming the stair-stepping effect caused by the layer by layer manufacturing. In classical method of stereolithography DMD structures are used to provide black and UV illuminated areas for the fabrication. Proposed method uses the grey-scaled images on the layer transition areas and decreases the observation rate and formation amount of stair like inter layer structures. (*Fig. 1.10*)

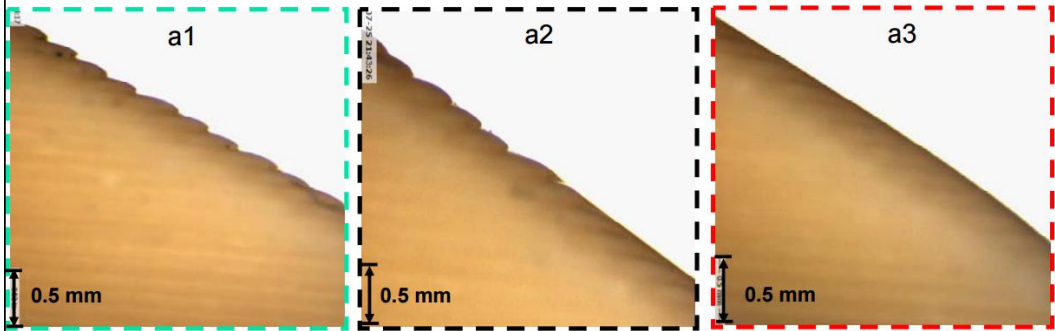


Figure 1.10: Decrease in the formation of stair like structures with grey-scale image projection technique developed by Pan. [27]

Problem of stair-stepping caused by poor surface finishing of stereolithography is a common problem as defined in the micro-stereolithography section. Ali [28] gets through this problem as defined in the system part of this research. Also

using the same developed stereolithography device of this research, application of continuous fabrication surface resulted in decreased topographical variation caused by the step-by-step fabrication. (*Fig. 1.11*) Decreased roughness profiles on the sides of the fabricated parts are useful in terms of increased manufactured quality and further application usages of the structures.

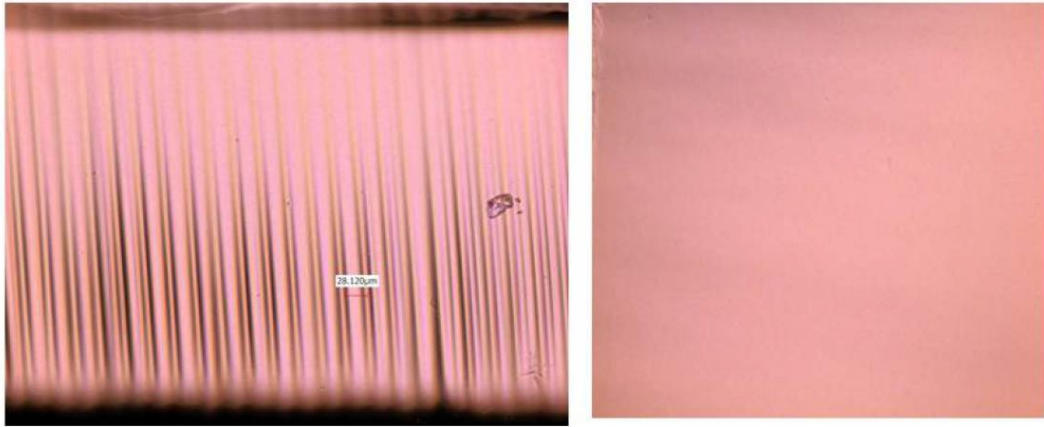


Figure 1.11: Layer by layer fabrication with the use of  $25 \mu m$  layer height and result of continuous fabrication platform motion usage. [28]

## 1.5 Motivation and Contributions

Fabrication trials made using the experimental process parameter optimization methods showed varying amounts of improvements on the manufactured products. Different system parameters like light intensity and fabrication speed are optimized in order to decrease the dimensional and structural errors in the parts when compared to the 3d Cad design models. For all different structures, optimization experiments are repeated in order to get the most accurate result. Small differentiations in the speed displayed significant changes on the fabrication process. Initial fabrication trials with some designs took up to 10 hours to fabricate with little information about the nature of the process. Apart from the time consumption of a single fabrication, multiple fabrications were needed to be made in order to define the parameters correctly.

Secondly, errors observed and measured on these fabrications have lots of similarities in common. These nearly identical differentiations from the desired cad design models on the solidified shapes, created some ideas about the compensation of the reasons creating the similar faulty areas even in totally different structures.

These faulty areas are mostly placed in the bottom and top areas of the 3d shapes. Because of the attenuation of light inside the liquids which is the most basic characteristic of the stereolithography during the fabrication process, after a specific layer  $x$  is cured and following layers starts to be solidified, the amount of energy applied to these following also increases the irradiation amount of the layer  $x$ . This causes an energy accumulation especially on the bottom surface of the fabricated part. This excessive amount of energy causes unwanted solidification on the bottom areas and prevents the fabricated part reaching the exact dimensions specified on the design. Also for the uppermost layers which are solidified at the end of the process according to layer by layer fabrication order, some of the top layers energy levels do not reach the amounts to be enough for being completely solidified. (*Fig. 1.12*) This also results in the errors of curing as some of the pixels located on the uppermost layers do not become solid. Condition for the upper layers is called as under-cured solidification and condition of excessive solidification on the bottom layers is called as the over-curing.

These type of errors caused by the undesired curing occurring on the fabrication surface create the need of solidification control with the adjustment of process controlling parameters. In the further chapters, sequential to the mathematical modeling of the process, simulations also showed similar types of errors. Also the results of trial and error based experiments induced the need of a more systematic way of dealing with the parameter optimization for the process. To start with, chemical explanation of the solidification needed to be examined carefully by defining the polymerization and layer curing mathematically. This could also lead the way for clear understanding of the importance about the system controlling parameters.

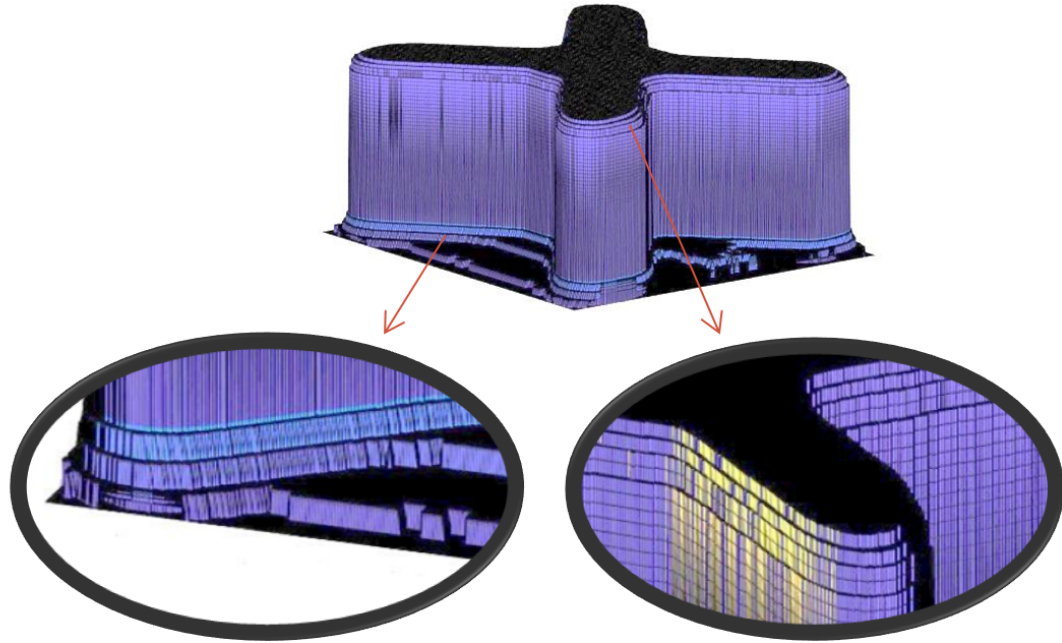


Figure 1.12: Over cured areas at the bottom and under cured areas at the top side of the structure

This thesis aims to solve the described over and under cure problem caused by the light attenuation inside liquid polymer resin during the stereolithography process. Layer cure model is explained and investigated for the established manufacturing system in Chapter 2 based on previous researches. Then with the definition of process parameter, proposed pixel solidification model is explained. This model investigates the polymerization and curing based on single pixels apart from the surface cure depth calculation in the literature.

Using the model and simulations, developed control algorithm is explained in Chapter 3. Iterative parameter adjustment scheme is described. Simulation and fabrication results are shown for the real life validation of the learning algorithm. Results section discusses that the proposed scheme is capable of decreasing the fabrication errors in varying amounts based on the shape and processing time. Possible future works, results of experiments and fabrications are evaluated in final Chapter 4.

## Chapter 2

# Mathematical Modeling

Mathematical modeling of curing process in stereolithography is an important way to explain the physical and chemical phenomena of additive manufacturing using a light source for solidifying a liquid resin material layer by layer. Many researches have been done to explain the UV-light based solidification and process planning studies are made to improve the quality of the manufacturing process. Improving the accuracy of systems control algorithm and increasing the complicity of the calculations before manufacturing a specific design for improving the build quality is also recognized as a way of creating a more advance process. Mathematical modeling of the complete process is the first step of understanding the nature of solidification. Using the model, a simulation scheme is developed for testing the control algorithm, eliminating the necessity of making a production on every step of the iterative control scheme. Layer cure modeling is the base for mathematically explaining the stereolithography process. It aims to calculate the depth of a single solidified layer during a production with specified parameters and a known layer image size. These parameters come up from the properties of the subsystems in the stereolithography setup. Main sub systems are the light source, material chemistry of the resin and positioning device. As some of the parameters were unknown due to the unique setup used in this research, various measurements and experiments are conducted to obtain all parameters. After the verification of parameters in the layer cure model, calculations are gathered

up for improving the model to a more complicated state. That state is proposed to demonstrate the layer by layer curing as it collects and combines the curing information for every layer and makes an assessment of the whole 3 dimensional manufacturing.

## 2.1 Layer Cure Model

Cure depth is the main parameter that defines the height of the area that is solidified inside the resin. Examining the relation between the light intensity amount on the surface and the desired layer height is mainly based on the cure depth equation. Cure depth of a layer can be found using equation(2.1) below. [29]

$$C_d = D_p \ln (E/E_c) \quad (2.1)$$

Where,  $E$  is the light irradiation dose which is called as the exposure ( $mJ/cm^2$ ). It is the energy received by a pixel (unit area) on resin surface.

$C_d$  is the cure depth which will be used to define the distance of curing so that the thickness of the layer produced can be calculated.

Now in order to find  $C_d$  it is required to find  $E$ ,  $E_c$  and  $D_p$  values of the desired system. The value of  $E_c$  and  $D_p$  are based on the resin which is generally provided by the commercial resin companies. But in this research, the mostly used resin is a self-prepared one with unique chemical properties. Therefore, as the resin has been prepared manually, these parameters are measured and calculated specifically. However,  $E$  value depends upon the light source that is used to cure the resin. That is the reason why a different measurement is made to get the valid exposure amount of the system.

The value of  $E$  can be calculated using following equation.

$$E (mJ/cm^2) = I (mW/cm^2) * t(sec) \quad (2.2)$$

Where  $I (mW/cm^2)$  is the irradiation amount of light source on the unit area, and  $E (2.2)$  is the exposure on the surface for a defined amount of time interval as shown in the formula.

For finding the amount of  $E$  on the surface, measurements are done based on the calculation of un-calibrated area exposure observed with the DSLR camera images. As explained in the equation, firstly it is planned to find the amount of irradiation on the surface by measurements, so that using the time interval on the manufacturing process, exposure value could be calculated and used in the other useful equations. From the camera images, it is possible to find the color intensity of each pixel with Matlab. Using that initial intensity values, secondly a calibration should be done in order to reach the total exposure and specific areal exposure on the image.

For calibration, the amount of actual exposure in the whole surface is measured in Advanced Research Laboratories in Bilkent with power meter. For a specific image and dimensions, total value of irradiation is averaged as  $30.6 mW$ . Total area of the image projected is also measured as  $4.16 cm^2$ , so the irradiation ( $I$ ) on the unit area is calculated as  $7.394 mW/cm^2$ .(Fig. 2.1)

Also, from the image taken with the camera, uncalibrated light intensity amount of all pixels are summed up with a prepared Matlab code.(Fig. 2.2) Actual surface exposure is then divided by the total of light intensities so a calibration constant  $k$  is found. Then it is possible to find exact exposure amount in every pixel by multiplying the intensity with that constant. The reason for this calculation is to correctly find the exposure for every pixel which will then be useful in the solidification calculation based on each pixel.

The depth of penetration  $D_p$  is a resin constant which implies the specific amount of light that penetrates into a measurable depth of liquid. As the constant was unknown for the self-made resin a testing was a need to calculate the

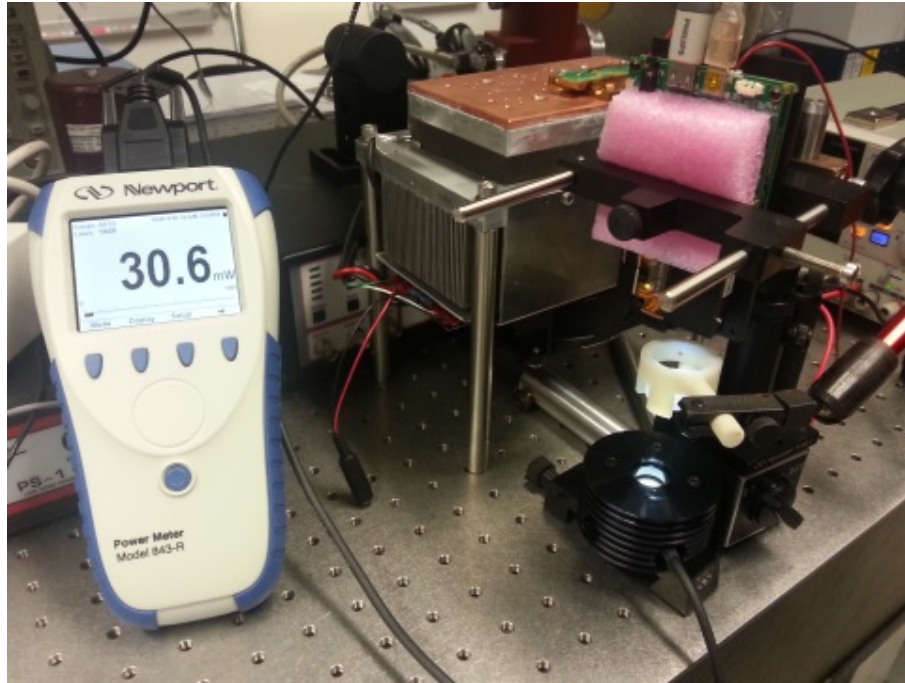


Figure 2.1: Power meter setup to find the irradiation of DLP projector.

amount. Using various equations to find the depth of penetration, firstly attenuation coefficient is found. Fourier Transform Infrared Spectroscopy is used for the measurement. This technique is used to measure the amount of absorption inside a material that can be in different states.(2.3) For the liquid state of the resin, transmittance amount is measured according to a wide spectral range at the end of the FTIR testing.

$$T = e^{-\epsilon l} \quad (2.3)$$

Where,

$T$  = the amount of transmittance which is the result of FTIR testing,

$\epsilon$  = is the attenuation coefficient

$l$  = is the thickness of the sample.

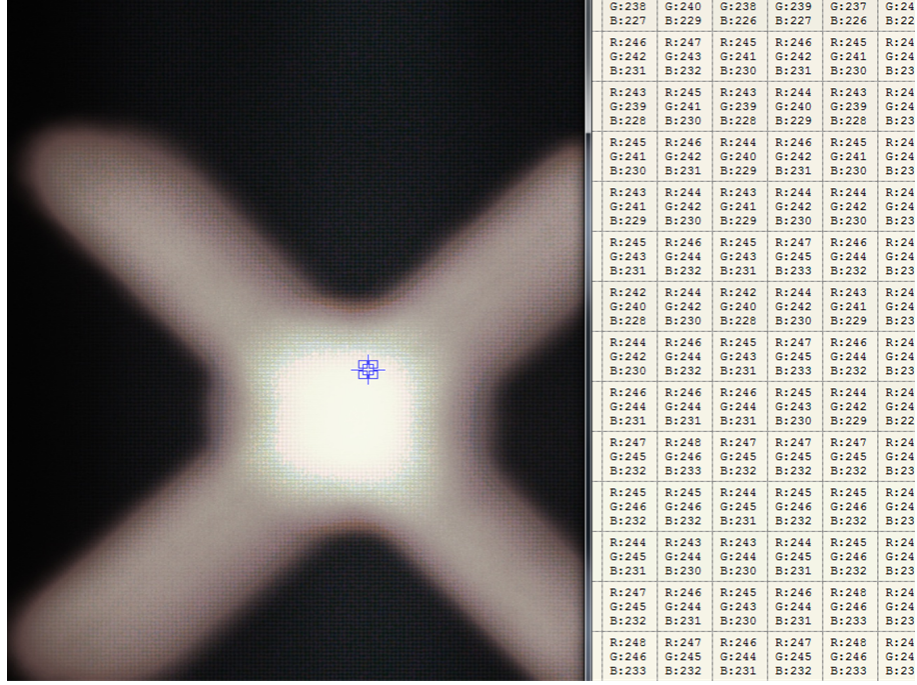


Figure 2.2: Pixel intensity values of a specific area.

In the experiment, sample thickness ( $l$ ) was taken as  $185 \mu m$ . Liquid resin is placed in a specimen between two special glass materials. Thickness of the resin which is the distance between the glasses is measured by a microscope for later use in the equation. DLP projector used in the system is also a part of the equation as the LEDs in the projector provides the light in a specific wavelength. From the user manual of the device, Young Optics DLP Lightcrafter, information about the effective color on the resin is found.

Using the attenuation constant found using the transmittance amount and sample thickness, penetration depth is found through;

$$D_p = 1/\epsilon \quad (2.4)$$

For the tested case, at  $460 \text{ nm}$  wavelength where DLPs blue light works, amount of transmittance is  $81\%$ .(Fig. 2.3) So  $D_p$  for the self-made resin is calculated as  $96,936 \mu m/s$ .(2.4)

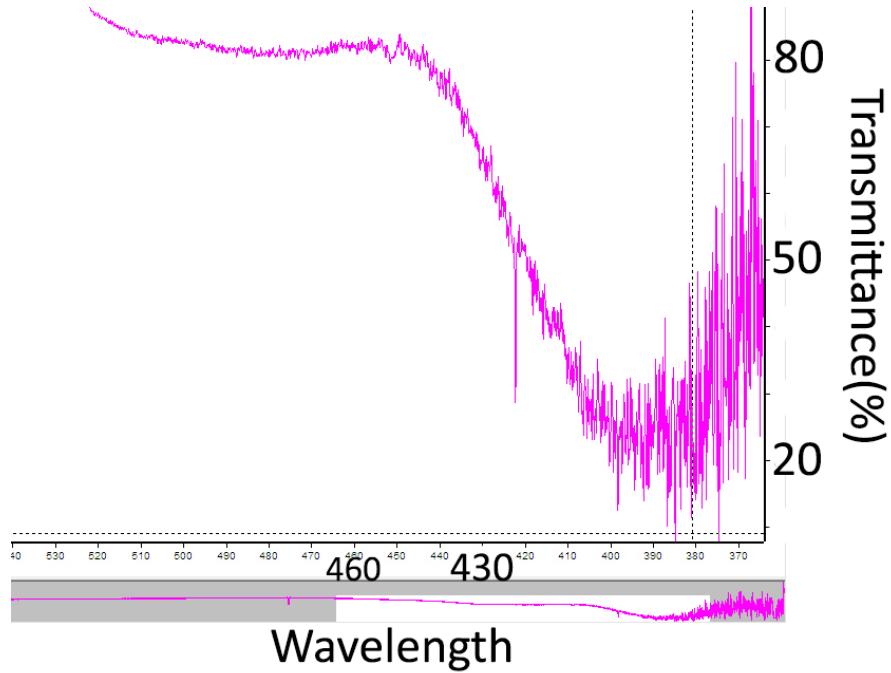


Figure 2.3: Result of FTIR testing, showing the percent of transmittance for different wavelengths.

Other calculations that will be used in the mathematical model are also listed. Exposure at specific depth  $z$  (2.5)[30];

$$E_z = E * e^{-z/D_p} \quad (2.5)$$

$E_{critical}$ , the amount of energy where the curing starts(2.6) is another important value for the calculation of the cured and uncured points for all pixelated areas;

$$t_{critical} = E_{critical}/I \quad (2.6)$$

$E_{critical}$ , could be found experimentally. For layers to bind each other, resin has to cure down to a depth of at least equal to layer thickness(2.7);

$$C_d \geq LayerThickness(LT), \quad (2.7)$$

$$D_p \ln (E/E_c) \geq (LT), \quad (2.8)$$

So minimum time of exposure for desired layer thickness  $(LT)$ (2.9);

$$t_{min} = (E_c/minI) e^{(LT/D_p)} \quad (2.9)$$

$$A = \varepsilon cl = \epsilon l \quad (2.10)$$

Where  $A$  is actual absorbance(2.10),  $\varepsilon$  is molar absorptivity (of attenuator),  $c$  concentration of attenuating specimens in material and  $l$  the path length which is the distance light travels through the material. For the  $N$  component mixture resin used for the production(2.11); concentration  $c_i$ , wavelength  $\lambda_i$ ,  $A(\lambda_i)$ is:

$$A(\lambda_i) = l \sum_{j=1}^N \varepsilon_j(\lambda_i) c_j \quad (2.11)$$

This calculation can be used for finding the absorbance of the self-made resin theoretically using the concentrations and absorptivity of each ingredient. Result of the calculation can be compared with the UV spectroscopy results for the specific wavelength. Cure depth formula is used for a reverse calculation for finding the critical energy(2.12) of the self-made resins. [30]

$$E_c = \frac{E}{e^{(C_d/D_p)}}, E = I * t \quad (2.12)$$

As mentioned before, an experiment is designed in order to find the critical energy of the resins. Firstly production platform is decided to be placed in different distances under the surface of the resin, leaving varying spaces for resin curing above the platform. That distances are taken as 1, 2, 3 and 5 mms.

Above 5 mm no proper resin curing is observed so longer distances are not taken into consideration.

Same shape of a  $1\text{ mm}^2$  square is reflected to the surface with constant amount of radiation and with the highest possible value of  $274\text{ mA}$  in terms of light intensity. Taking that constant amount was needed as from the previous measurements, DLP projector is characterized using these parameters.

Exposure time is taken as another variable from the formula and varied between 15 to 180 seconds. For most of the trials values lower than 15 seconds did not caused any resin curing and above 3 minutes cured shapes started to be inconclusive for the measurements.(*Fig. 2.4*) At the end of productions the thickness of the produced shapes are measured which theoretically gave the cure depth value for the known amount of exposure time and light intensity.

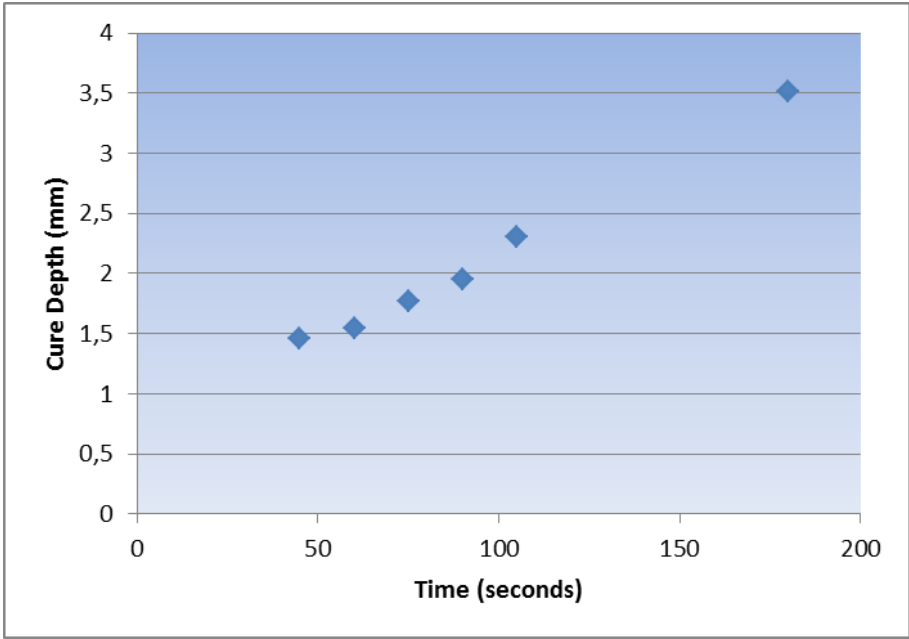


Figure 2.4: Results of experiment with platform at distance of 5mm and exposure time from 45 to 180 seconds.

As depth of penetration is a previously measured resin property and also the amount of radiation that projector gives is also calculated, the only unknown became the critical irradiation on the formula and average values are calculated with Matlab processing.(*Table B*)

Table 2.1: Results of critical irradiation experiment

Experiment (Platform Distance)	Critical Irradiation
1 mm	7.326
2 mm	7.2115
3 mm	7.2606
4 mm	7.2941
5 mm	7.2366

Through all calculations and averaging of the results, value of critical irradiation is turned out to be  $7,266 \text{ mJ/cm}^2$ .

When it is compared with the already known critical energy amounts of the other used commercial resins which are slightly more than  $10 \text{ mJ/cm}^2$ , it can be commented that self-made resin can be cured faster with the same amount of energy and commercial resins having properties like elasticity and high hardness requires more energy for the process.

Validation of the pixel cure model on the system is done within the context of thesis written by Ali. [28] Fabrications and measurements of different structures are made in order to verify the application of model on the setup.

## 2.2 Process Parameter

Stereolithography system designed is defined with a working scheme difference when compared to the other commercial devices. In classical technique, fabrication platform makes a step by step motion for layer by layer fabrication. Established systems fabrication platform makes a continuous motion downwards in order to create nearly layerless structures and for increasing the fabrication quality. Therefore from the process parameters defined in the cure depth modeling of the system, exposure time becomes meaningless with the usage of continuous motion. Also instead of the exposure time for each layer, a fabrication speed is defined for each interval in the developed model.

A pixel cure model is proposed in the following chapter, defining the general motion again with intervals of varying heights. These spacings could be taken as layers but for decreasing the layering effect which could be observed in the measurements, interval thickness values are defined as small as possible so the layer number is increased from 50-100 to 5000-10000. For a part with 5 *mm* height, normally layer thickness of 0.1 *mm* is used, but with the proposed algorithm this value is decreased to 1  $\mu m$ .

## 2.3 Pixel Cure Model

Calculation of the solidification amount and time of the liquid material is the main aspect of the error calculation and correction of the iterative learning scheme. For creating an iteration based error decreasing algorithm and avoiding spending too much time with the fabrication trials, a model is prepared and process results are simulated on Matlab. Model depends on the cure depth calculation and Beer-Lambert Law previously explained. The amount of irradiation reflected on fabrication surface with the projection, creates a light exposure on the surface. Exposure is dependent on the time interval that the resin surface is kept irradiated.

During the process, light entering the resin from the uppermost layer starts attenuating inside the liquid and causes a logarithmic increase in the exposure amounts of the underlying layers, which results in the over-curing of the previously solidified layers. Attenuation of the light rays inside the liquid material is explained mathematically by the Beer-Lambert Law. Therefore, when it is used with the polymer resin curing process with the adopted formula, it provides the calculation of the attenuated amount of energy at a specific point inside the resin.

Secondly, cure depth calculation is an important part for the clear understanding of the chemical process. Cure depth formula defines the height of the area cured with application of a specific amount of exposure and with material constants; critical exposure and depth of penetration. For finding the exposure on

the fabrication surface, a DSLR camera is placed on the process area and layer image projected is recorded. Using the main light intensity value previously found by power-meter, recorded uncalibrated pixel color values are adjusted accordingly in Matlab to give the exact light intensity on every x-y axis point of a layer.

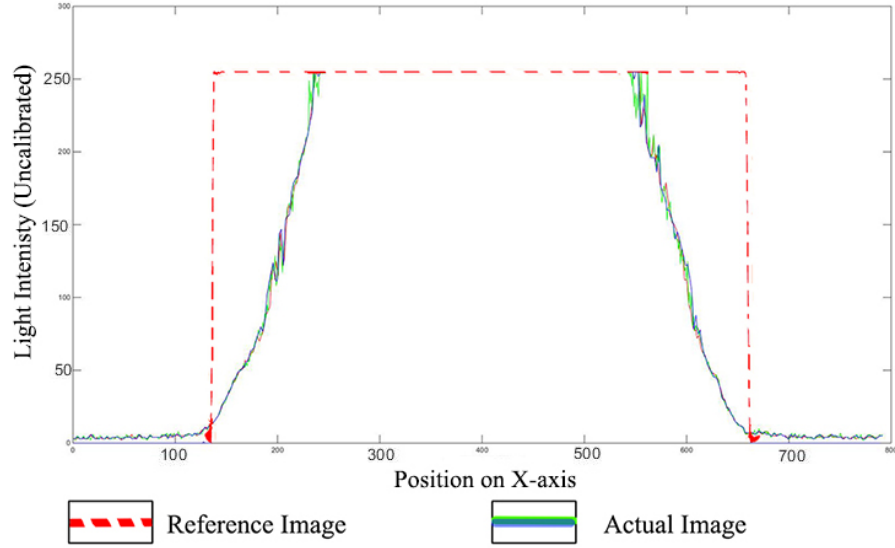


Figure 2.5: Intensity difference between the reference and actual irradiations.

Main idea behind the solidification model used in this research is based on the critical exposure and summation of the logarithmic increasing exposure on a specific point of the liquid according to intensity variation.(*Fig. 2.5*)

Model defines the fabrication area by layers having specific heights in z-axis and by pixels, indicating points in the x-y axis. Given a specific area for projecting, irradiation per unit area is found as  $7.394 \text{ mW/cm}^2$ .(2.13) This value is then used for finding the total or areal exposures on varying profile images. Using this representation, a type of mesh is created specifying the instantaneous exposures of every point inside the 3d volume of the liquid container. Logarithmic summation of the irradiation(2.14) that will be used in the simulation algorithm is based on that unit time single layer mesh value. When the irradiation on the mesh unit exceeds the critical exposure in a defined time parameter,(2.15) solidification starts. When the exposure is increased to a larger amount than cure depth, that unit is counted as solidified.(2.16)

$$I_{unitarea} = \frac{I_{total,measured}}{I_{total,uncalibrated}} * I_{avg,pixelvalue} \quad (2.13)$$

$$E_{x,y,z} = I_{unit,x,y} * t_{exposure} + e^{-l*z/D_p} \quad (2.14)$$

$$E_{x,y,z} \geq E_{critical} \succ \text{Curing starts at } x, y, z \quad (2.15)$$

$$E_{x,y,z} \geq C_d \succ \text{Cured pixel at } x, y, z \quad (2.16)$$

$E_{critical}$  shows the critical amount of energy for the start of the solidification as discussed and calculated in layer cure model.  $E_{x,y,z}$  defines the amount of exposure of a point or so called a pixel located at coordinates x, y, z. For finding the value of  $E_{x,y,z}$ , formula of exposure at a specific depth is used with varying irradiation amounts of different pixels on x, y axes.

Pixel cure model is the basis of fabrication simulations and possible error calculation with the comparison to the desired irradiation image. Model provides a detailed evaluation of the single pixel oriented solidification process for stereolithography. A fabrication of a structure including 1000 layers and more than 300.000 pixels just on a single layer creates a huge amount computational work for calculation. For the following section of the thesis, this evaluation process is repeated couple of times for each iteration. Therefore, with the use of an effective coding architecture, simulation time intervals are tried to be kept in the minimum level.

# Chapter 3

## Development and Validation of the Control Algorithm

### 3.1 Iterative Learning Control Algorithm

Correction algorithm that was created in order to decrease the error amount of the additive manufacturing fabrication is based on the error summation of the x-y axis mesh points on a single layer. According to the total error over each layer, a new corrected fabrication speed is assigned differently for each layer. An error based parameter correction model is created in a previously conducted research as presented in the following section.

#### 3.1.1 Single Layer Based

At the start of the scheme, reference 3d model is placed on the slicing algorithm for determination of layer shapes according to the desired layer thickness given as an input. Then using the thickness data, in coordination with the positioning controller, defined layer shapes are projected through the DLP projector to the fabrication platform of the system.

Main input for the iterative learning algorithm is the reflected layers image on the manufacturing platforms surface. But before the use of the actual reflected layer as a direct input, a desired structure is used to create a reference layer description. That reference layer structure is the result of an imaginary layer curing based on a perfect reflected layer shape assumption. This form is called as the desired or reference image. Using these desired images for each layer of the whole shape, a simulation code generated on Matlab is used to manufacture a digital 3D structure.

Projection of the light to the manufacturing surface depends on various conditions like the reflections caused by outer light effects and errors due to the optical system. These variations result in the imperfections of the projected image when compared to the exact specifications of the desired irradiation amount specified differently for each pixel located in the surface.(*Fig. 3.1*) Matlab utilizes the layer images as an input with the use of a CCD camera, as the layer image reflected through the projector and the optical components is recorded with the camera placed on the production surface. That recorded sight of the layer reflection is named as the actual layer image. Average profile positioning of these images are shown below.

Classical stereolithography applications works on a single exposure time value that is applied to all layers in the same way. In this researches case, for reaching a smoother surface fabrication and faster processes, position controller uses the time and layer thickness parameters for calculating and applying the process speed per layer. Apart from that conventional method, single layer based algorithm aims to vary the fabrication speed per layer values for reaching better process and detail quality. Base method only compares the desired speed with the actual speed of the platform and adjusts the command for reaching desired value. Iterative learning algorithm works on the base of an error calculation. Difference between the actual layers image data from the previous iteration is measured by making a comparison with the desired image data fed to the algorithm. The difference determining the dimensional error amount on the layer creates a correction factor on the speed values of that specific layer in the following iteration. Correction factor speeds up or slows down the motion of exposure at that layer during the

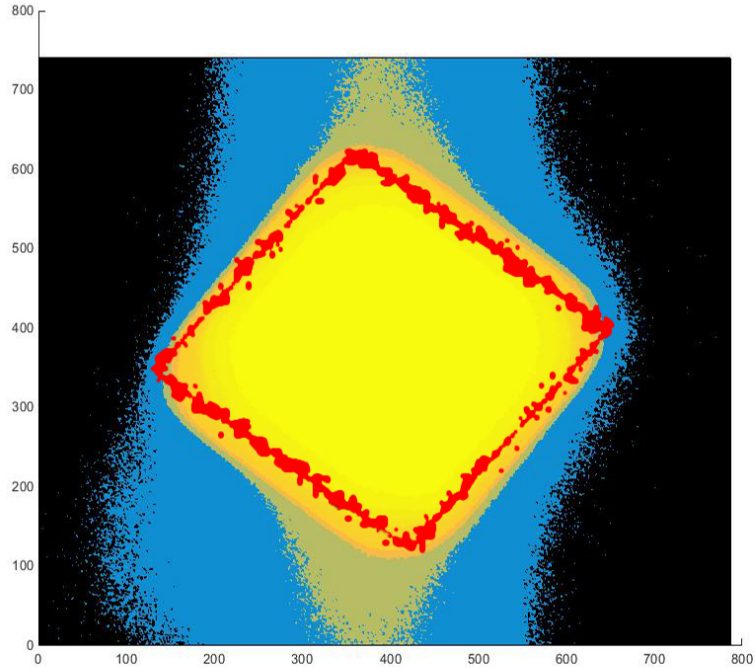


Figure 3.1: Expected versus real life energy distribution on surface.

next iteration. Learning algorithm uses couple of primary inputs for the reference and actual image structures which are compared using the simulations.

Firstly, using a perfect reference layer image, a 3d structure in exact desired dimensions is created in Matlab environment including all the mesh data. Reference structure is the one to be compared as the main model. Secondly, actual structure simulation is made. According to the projected layer image, simulation of fabrication process is done in detail and 3d model is created virtually. That model also has all the mesh data indicating the cured or un-cured pixels of each layer modelling the real life process directly. Data of the trial fabrications that will be examined in the following parts of the paper includes nearly 150 million curing information of each pixel for 3d structure composed of 600 layers with dimensions of 5:5:6(width, length, height) mm.

Finally the error calculation algorithm starts working as it compares each pixel of the reference and actual model by defining a positive error value if the desired

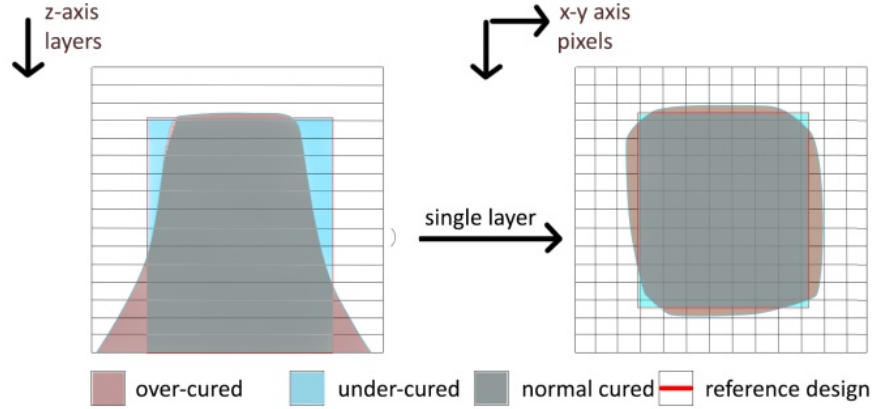


Figure 3.2: Example mesh data on x-y-z layers for simulation of over-cure and under-cure errors.

model is not cured but reference indicated that according to the desired model, pixel should have been cured.(3.2)(Fig. 3.2) Opposite of that happens when the actual model is cured but reference indicates that it should be un-cured which means this single pixel is over-cured.(3.3) If the actual and reference models agree that the pixel is cured or un-cured as desired, algorithm does not make any change in the error amount. By the addition of the error values of pixels, a total error value is appointed for each layer.(3.4) If the total error is negative it means most of that layer is over-cured so the exposure amount given to that layer should be decreased accordingly in the following iteration. As the error calculation is done for the whole body by the step-by-step layer checking, according to the performance comparison between two models, layer based velocity command of the new iteration is applied as a function of time and layer thickness.(3.5) Gain of the adjustment algorithm is defined with  $y$ .

$$E_{x,y,z,reference} = 1, \text{cured} \quad \text{or} \quad 0, \text{uncured} \quad (3.1)$$

$$E_{x,y,z,actual} < E_{x,y,z,reference} \succ Err_z + 1 \quad (3.2)$$

$$E_{x,y,z,actual} > E_{x,y,z,reference} \succ Err_z - 1 \quad (3.3)$$

$$Err_{total} = \sum_{z=0}^l Err_z \quad (3.4)$$

$$t_{exp,z}^{i+1} = t_{exp,z}^i + y * Err_z \quad (3.5)$$

Block diagram given below explains the interaction between the learning algorithm based on the exposure time value of the system and controller of the positioning system for vertical movement of the production platform. (*Fig. 3.3*) Layer thickness amount and the overall layer shapes are interpreted with the use of the initial reference shape firstly given to the algorithm. Using the data of the desired layer thickness for each layer, reference positioning command is fed to the position controller. Also the desired layer shape is projected through the data applied on the DLP projector light source.

The velocity input is provided using the data of the current position of the platform and input of the velocity calculation algorithm. Therefore, a smooth movement for the platform and nearly layerless manufacturing of the desired part can be reached.

In conventional working scheme of the velocity controller of the platform, difference between the actual working velocity and the desired velocity are compared to create a control command for the manufacturing area movement velocity. When the iterative learning algorithm is used for this process, a dimensional error of the produced part is calculated beforehand, based on the difference of desired and actual layer images of the previous iteration. (*Fig. 3.3*) That difference creates an error value for the iteration on that specific layer. Taking both the previous and upcoming layers error amounts into consideration too, the error for that specific layer is used to manipulate the motion of the manufacturing platform. A correction term which would slow down or speed up the platform velocity is created, for adjusting the exposure amount by increasing or decreasing the exposure time respectively at that layer. As shown below, a correction trace is created for all iterations.

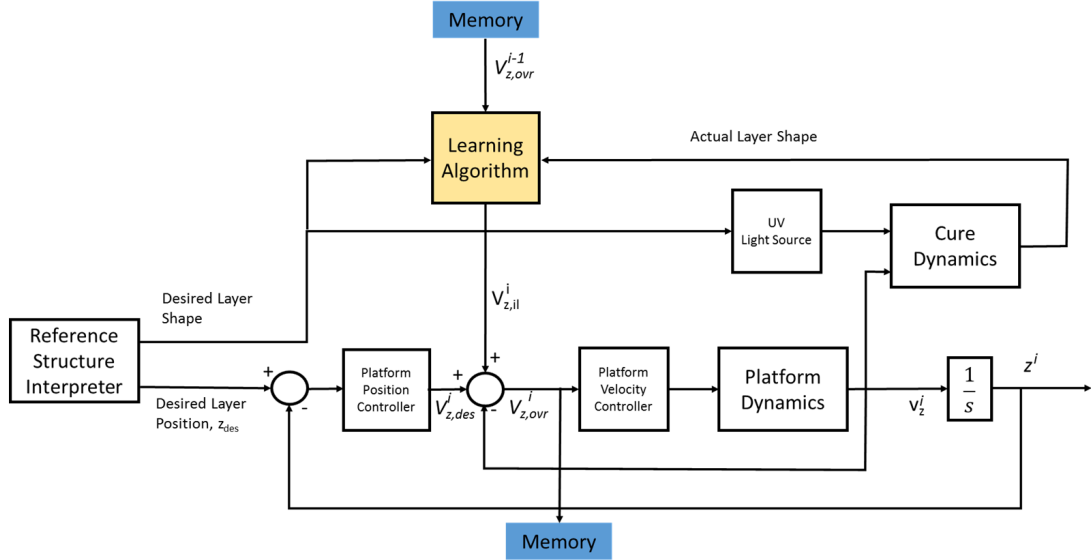


Figure 3.3:  $\mu$ SLA System block diagram.

Using the new assigned command values, exposure quantities are re-calculated and fabrication is done again in the simulation environment. Therefore instead of using an on-line measurement or observation on the system, differences are calculated and changes are made off-line by the use of fabrication simulations. Then the process goes on the same way when compared the starting iteration as error values are calculated again using the mesh valuation and new parameters are formed in the following iteration loop. Aim of the trials is decreasing the error in minimal amount of iterations and figuring out the ultimate speed parameters.

All iterations are based on the adjustment of layer exposure time so the layer specific fabrication speeds for decreasing the total amount of error on the 3d structure. Single layer based algorithm works layers based, as the error value of a specific layer is taken and applied on the correction formula by multiplication with a single gain value. Therefore each layer's parameter is changed without considering the errors or changes in another layer. For improving the performance of error decreasing logic based on the mathematical representation of the chemical process, a more complex algorithm scheme is created in the next section.

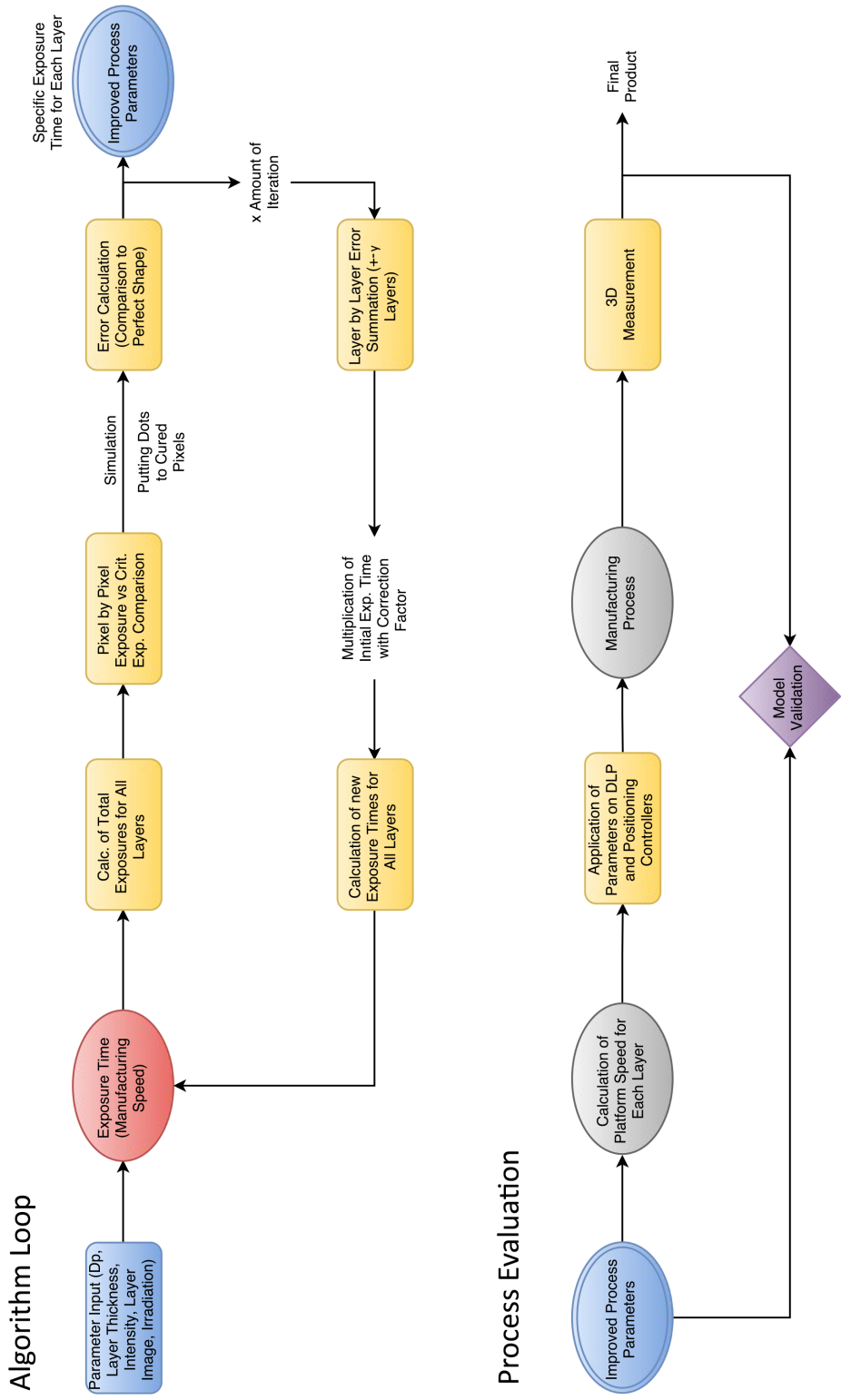


Figure 3.4: Diagram of iterative learning scheme and fabrication process.

### 3.1.2 Advanced Multiple Layer Based

Algorithm presented in the previous section represents a basic error correction algorithm on single parameter adjustment for each layer. A secondary algorithm using the logic derived from the operational order of the chemical process is created for increasing the effectiveness. Attenuating nature of the light rays creates an additional effect on the exposure amounts of each layer which is also the main reason of the over curing phenomena. For overcoming this effect, algorithm is improved to affect exposure amounts not only based on the single layers error values but with the addition of multiple previous layers error amounts for creating a combined error variable.(3.6)

$$Err_{avg}^z = \left( Err_z + \sum_{l=z-a}^z Err_l \right) / a \quad (3.6)$$

Decreasing the amount of over-curing for a layer creates the need of decreasing the exposure amount of that specific slice. While doing this in the basic algorithm, effect of the previous layers is neglected and control scheme multiplies the error with an experimentally adjusted gain. However the improved scheme takes an average of the error amount for next '*interv*' (3.7) layers of the fabrication simulation and considers that average value in the new parameter creation for the next iteration. (3.8) Due to the attenuation of light, following layers in the fabrication order are expected to have more over-curing. This makes the new algorithm calculate a higher error amount on a specific slice when compared to the primary scheme. Increased amount of error cause sharper changes in the layer-specific speed values and algorithm acts more in less number of iterations.

$$d = 1, 2, \dots, interv - 1 \quad (3.7)$$

$$t_{exp,z-d} = t_{exp,z-d} + * \left( \sum_{l=z-a}^z \frac{Err_l}{a} \right) * (interv - d)^c \quad (3.8)$$

Apart from the average error calculation, also the effect of these values on the process is aimed to be increased. For this purpose, when the algorithm is dealing with a single layer using the average error, exposure amounts of the previous layers are also modified accordingly. Instead of only increasing the fabrication speed and applying a lower amount of exposure to that specific layer interval, previous layer exposure amounts which are gradually increasing the total irradiation application time on that specific layer are desired to be differentiated. Variation algorithm proposes a logarithmically decreasing effective change on the exposure amounts of the previous layers. So apart from the exposure time variance caused directly from the error on that specific layer, an additional change caused from the errors of the upcoming layers is also applied on the improved algorithm. (Formula above) This proposed algorithms logic is derived directly from the exposure calculation formula for a single layer. When the total exposure for a single layer is calculated, it is found as the sum of the attenuated exposure effects of previous layers and the actual exposure applied during the fabrication of that specific layer. Therefore, for decreasing the total exposure on that layer, just decreasing the irradiation application time on a single layer interval is insufficient and multiple layers parameters are adjusted to decrease error in minimum amount of iterations.

## 3.2 Simulations

Simulation trials are made with single layer based primary algorithm. These trials are used to guide the further validation tests of the multi-layer based iterative learning algorithm which includes the real life fabrication of the primary and final iterations.

### 3.2.1 Basic Shape

According to simulations planning, initial trials on the simulations are done with a simple square prism with  $5*5$  *mm* base dimensions and  $6$  *mm* height. All of the

trials are done with the slicing of the cad design into 50 layers. Simulations for each layer, calculating the amount of over or under-curing of these layers uses the layer amount as one of the main inputs. Simulations for the basic shape is done with the reference image digitally created which is also referred as the desired design. Secondary image is the one that is taken from the actual reflection of the DLP's projection on the fabrication platform. This image is referred as the actual images because it represents how the layer image is actually causing the solidification of the liquid resin on the surface.(*Fig. 3.5*)

Simulations made with the initial shape is done in 5 iterations but also considering the very first digital fabrication as the 1<sup>st</sup> iteration, which is the one made with a single process parameter for all layers. Using the pixel cure model calculations, total error amount of iteration sums up all wrongly cured and solidified pixels of all 50 layers. Error amounts of individual layers effects the amount of process parameter change in the following iteration with the use of the correction trace, which is previously mentioned in the iterative learning algorithm.

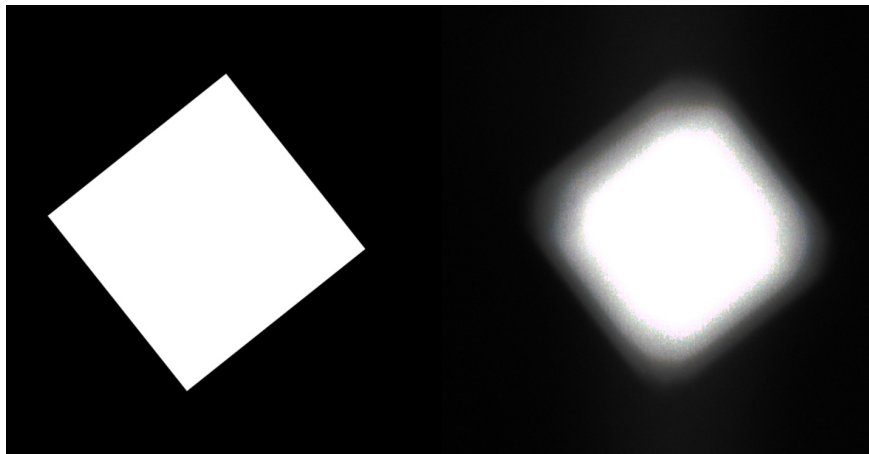


Figure 3.5: Reference layer image and projected layer image.

Pictures above show the reference and actual images that are entering the simulations as layer image projection inputs.(*Fig. 3.5*) It can be observed that effect of the optical system causes the undesired distribution of the light especially on the edges and corners of the desired shape. This condition also causes varying amounts of irradiations on different points of the surface which results in curing errors combining with the light attenuation inside the liquid resin.

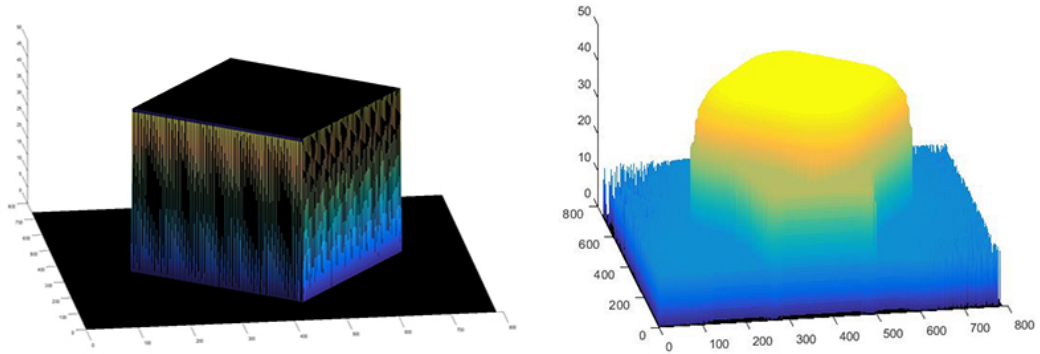


Figure 3.6: Reference and simulated structures created with the process simulation algorithm.

Results of the primary iterations are shown in the visualizations of the simulated fabrication. (Fig. 3.6) Shape of the reference is driven from the simulation only for one time, as it defines the perfect desired shape and not changed with increasing number of iterations. Shape of the actual fabrications structure, shows the over and under-cured areas in an exaggerated manner. Error is aimed to be decreased with the use of the algorithm as process with the use of single parameter results in huge amounts of over cured pixels at the bottom and under-curing at the uppermost side of the part.

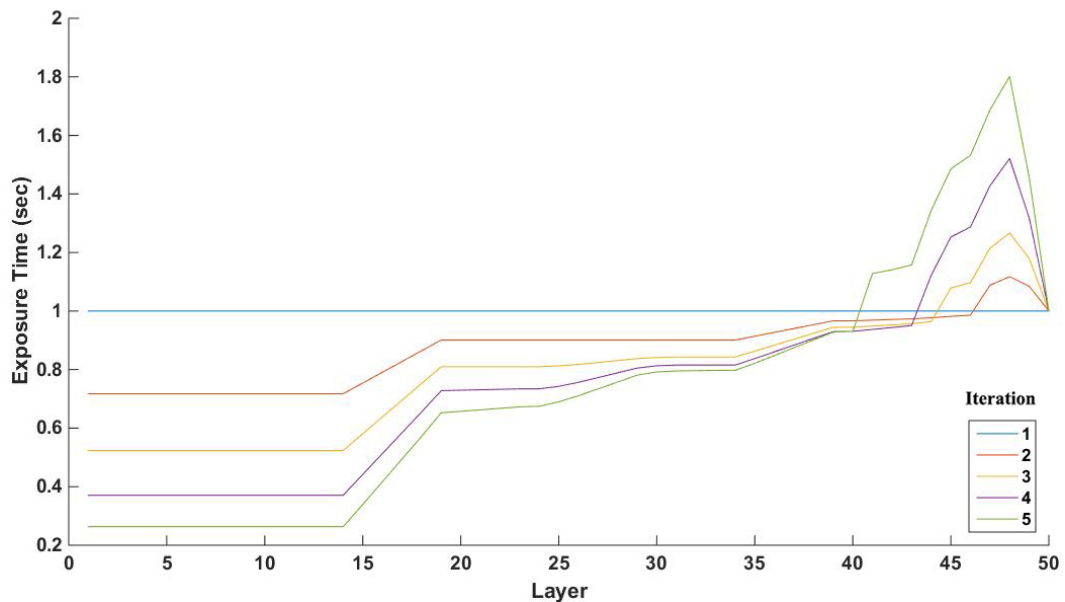


Figure 3.7: Layer number vs exposure time graph.

Graph below shows how the exposure time parameter changes with increasing number of iterations.(Fig. 3.7) This does not mean that the movement of the fabrication platform is step by step and layer by layer curing is done with fixed amount of exposure times. This represents the time that the continuous movement of the fabrication platform takes to pass the previously defined imaginary layer intervals. It can be easily observed that with increasing number of iterations, algorithm changes the exposure times in order to decrease the error.

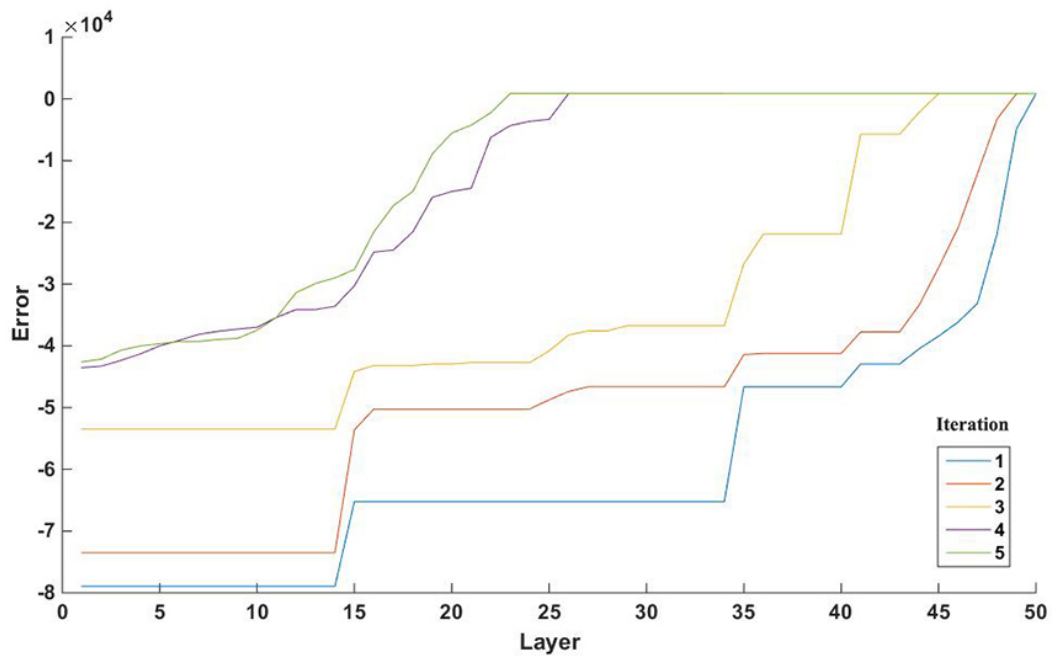


Figure 3.8: Layer number vs error graph.

From the final error distribution graph of layers with iterations, it could be observed that the error amount decreases and gets closer to zero.(Fig. 3.8) In each iteration, according to the error value of each layer interval, algorithm changes the exposure time which leads to varying amounts of errors for a specific layer. Algorithm decreases the error amount nearly 75% in this initial trial simulation of the basic shape.

For the top layers where under-curing of the structure is observed the error amount is drawn slightly above the 0 line. There could be 2 main reasons for this observation. One can be defined as although the exposure time is increased

on iterations to provide more light for desired solidification as it can be seen from the exposure time graph, because of the insufficient effect provided by this specific correction gain, desired amount of irradiation and total exposure could not be reached and under-cured layer seems to remain the same at the end of 5 iterations. This could be solved with the use of another gain value, but an optimum value is decided and kept throughout the whole initial simulations. The other and logical reason could be the dimensional errors on the image input preparation which could also cause that type of an error. Possibly caused by a small dimensional miscalculation on the actual image, that layer shape might be slightly smaller. Even though the algorithm tries to increase the exposure time to reach that dimension, as it could never reach the exact size, that would lead to convergence of the algorithm result into a value higher or smaller than 0. This could be negligible when compared to the error change amounts of the other layers.

### 3.2.2 Complex Shape

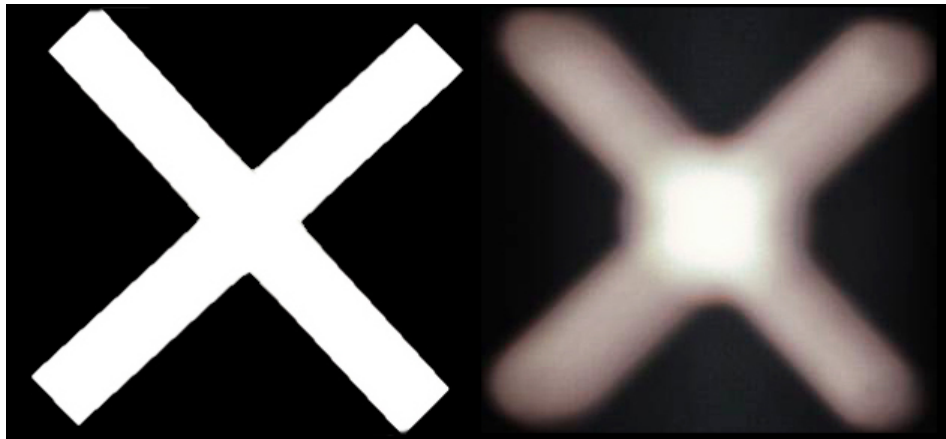


Figure 3.9: Expected vs actual layer projections on the surface for complex structure.

Initial trials went on with a more complex shape because of its structure. A cross shape is given as an input to the simulations with same amount of layer thickness and layer number when compared with the basic shape. Main difference was that the legs of the cross were narrow which causes less amount of light to

cluster on the center area.(*Fig. 3.9*) The huge solid structure of the basic shape causes larger amount of energy to yield at the center and distractions only happens in the outer edges.

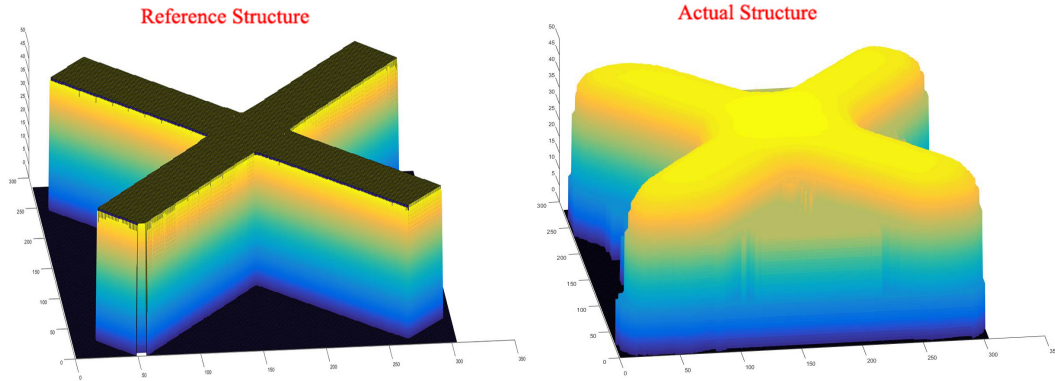


Figure 3.10: Simulated fabrications for complex shape.

Use of the primary single layer based algorithm resulted in up to 40% error decrease in the complex shape. This is mainly caused by the higher amount of edge length on this structure and increased number of sharp and edgy areas.(*Fig. 3.10*) Taking this information into account, new designs are used in the validation tests including the real life fabrication with the adjusted process parameters found through the correction algorithm simulations.

### 3.3 Validation of the Algorithm

Validation of the developed control algorithm on the system by measurement of the effectiveness of control scheme is an important part of the research. All modelling and simulations based on the model is done according to the parameters of the established stereolithography system. Therefore, an experimental design is made to prove that the fabrication quality could be increased in considerable amounts with the use of the iterative learning algorithm adjusting the speed parameter for the fabrication process of varying shapes.

### 3.3.1 Experimental Design

Experiments for the validation of the algorithm is based on the running of the learning iterations on the solidification and error calculation model presented. Therefore, an off-line control algorithm is used with the use of the simulations. Starting with initial fabrication parameters for every layer, error calculating simulations are done for adjusting the new parameters with following iterations. Measurements of the shapes are based on the validation of structural integrity of the part. Dimensions of the over-cured, under-cured areas and also irregularities on the basic structural properties of the desired shapes are measured for observations and comparisons. Various shapes are used in the trials in order to validate the algorithms effectiveness. A basic shape of a cube with previously defined dimensions, which is expected to show both over and under cured areas, is taken as the initial test structure.

Then according to the previous fabrication experience with the system, shapes like stairs or cavities inside the parts are determined to be hard to fabricate with the use of the classical method. Therefore, cad designs including these types of structural properties are made in order to be used in the simulations and iterative learning scheme.

Results are decided to be compared according to the amount of change in the error amounts of the fabricated part, when compared with the desired reference structure. Simulation algorithm is calculating the error amount according to the incorrectly cured and solidified pixel number on each layer and giving a total error percentage change in all iterations. This decrease of the heights on both under and especially over-cured areas on the structure are also shown in terms of error percentage in order to easily compare the fabrication results before and after the usage of the algorithm.

### 3.3.2 Basic Shape

Manufacturing trials for the algorithm have been done in the basis of testing the systems capabilities. Therefore, firstly the algorithm is used and tested for the calculation of ideal process parameters of a simple shape. Firstly, a simple cubic shape is aimed to be fabricated in order to observe the fabrication accuracy without the use of the algorithm. Using the previously made research about finding the optimum process parameters to get the best fabrication results possible, a starting speed parameter for the process is defined. This defined parameter is then put on the algorithm for further usage and calculation of the speed for every layer interval in the process.

Simple shape is defined without any curvatures or indentations so even before using the algorithm, over cured areas could be easily observed and the improvements could then be measured. For comparing the differences in the part quality, firstly a fabrication without the algorithm is done, using a single value of exposure throughout the whole process. The results are measured and dimensions of the fabricated part are noted. This part could be noted as the initial fabrication. (*Fig. 3.11*)

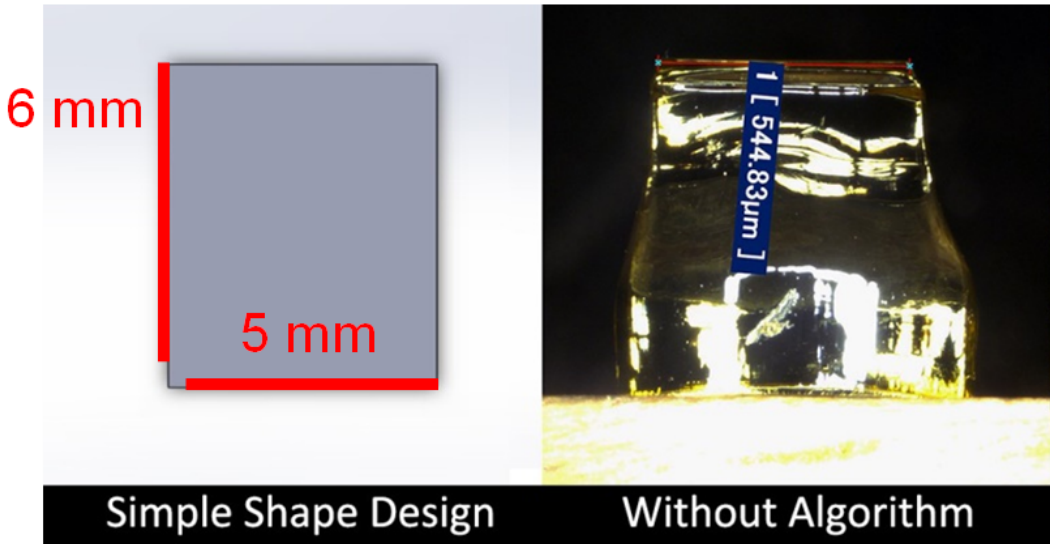


Figure 3.11: Initial fabrication of the simple shape design with the desired CAD model.

Then secondly, the layer image taken beforehand is applied on the iteration scheme for the new parameter calculation. At the end of 6 iterations, renovated speed values varying for each and every layer is defined. As defined in the algorithm section, changing scheme assigns a new exposure time to every layer according to the information that this layer is whether over or under cured in the previous simulation. Then these time values are changed into speed amounts using the layer thickness information. Speed values defined on Matlab using the algorithm are manually applied to the positioning systems software. Positioning system works on the basis of a classical manufacturing platform and software could adopt a g-code which enables the user to define varying speed parameters in different stages of the fabrication.

With the use of the parameters defined at the end of 6 iterations, a final fabrication is done for testing the error decreasing algorithm. (*Fig. 3.12*) First results are taken from the algorithm in terms of the decrease in the error as the simulation based on the mathematical model is used to calculate a theoretical amount of error decrease. Use of different learning gains resulted in varying amounts of error decreases. An optimum value for the gain resulted in the decrease of error amount up to 40% which shows the improvement of the fabricated parts quality and closeness to the desired shape. Then the results of the real life fabrication, processed with the same parameters used in the simulation are taken with the dimensional measurements made on the optical and laser microscopes.

### **3.3.3 Complex Shape**

More fabrications are planned and realized as it is necessary to prove that the algorithm is capable of decreasing the error amount in case of the fabrication of various shapes as the established additive manufacturing device should be ready for efficient fabrication of any given shape under the dimensional constraints of the workspace. Also these trials are used to determine the algorithms and systems capabilities. The initial basic shape is the representation of a structure which includes only a single over and under cured area. It is used for general testing

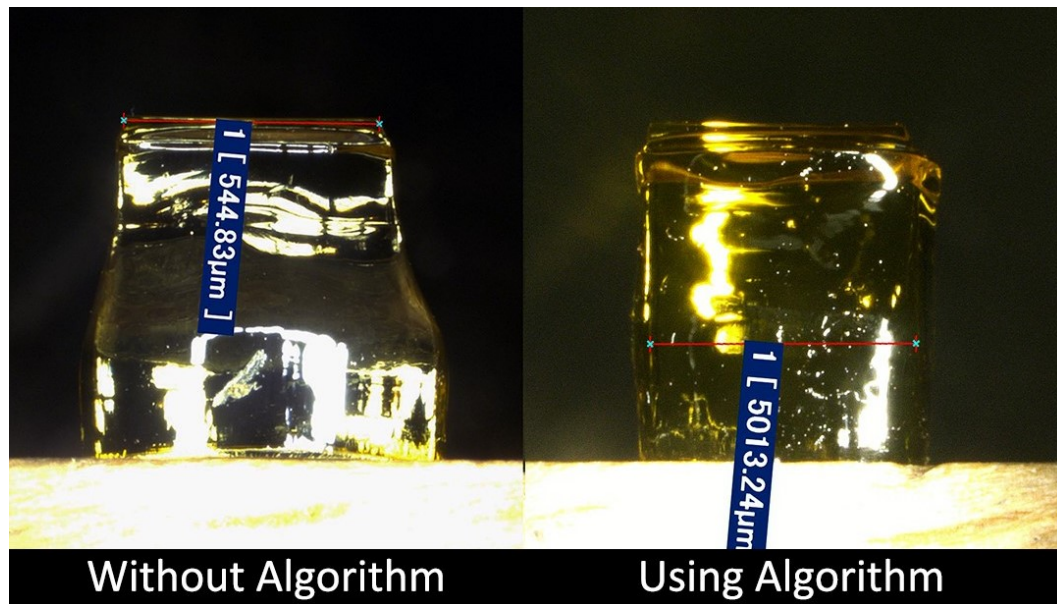


Figure 3.12: Fabrication results of the basic shape with and without using the algorithm.

of the control scheme in decreasing the error amounts of the large defected areas with a total height of 6 mm. Further shapes for the experiments are designed to include multiple over and under cured areas again inside of the same total height. Therefore, indented areas and holes are added to the initial design which will create more difficulty to the system in accomplishing structure variations with smaller dimensional changes.

As expected in the simulations, a higher amount of error is observed in the fabrication of the complex shape designs. Without the use of the correction algorithm and use of a single exposure value for all layers, manufactured parts includes more over cured areas in total. The initial parameters for the fabrications are determined according to the previous manufacturing experiments that were done for the fabrication of larger parts which includes fewer details.

Experimental parameter adjustment methods were used for these previous uses of the stereolithography system, which roughly succeeded in reaching better quality structures. Main problem of these methods was the high process time consumption as multiple amounts of fabrications should be done in order to get the

optimum parameters. Even then the perfect details were hard to reach because of the over and under curing on specific areas on the structures. For a single design, it requires multiple fabrication trials to reach the best possible parameters so; also high amounts of materials are used unnecessarily for the experiments. Use of the error decreasing algorithm and model based simulations get rid of the need for high number of fabrication trials for increasing the process quality, as simulated iterations are used instead.

An example of fabrication is formed through the need of creating holes or cavities on larger solid bodies. Micro-sensors or sensor housings could be fabricated with the use of similar designs. Therefore a design including a 1mm radius hole inside 5x5x6mm body is created and fabricated both with and without the advanced algorithm.

Without the algorithm, process failed to fabricate the desired shape with the use of a single exposure time for all layers. Bottom part showed large over-cured areas and the hole that was expected to be 6mm was all filled from bottom to top, but only leaving a roughly 1 *mm* deep cavity on the top side. With the use of that single parameter as the starting point of the algorithm, at the end of 4 iterations another fabrication is done. (*Fig. 3.13*) Using the simulation on all iterations, each of the total 600 layers had assigned a different speed parameter for itself.

Measurement of the fabrication showed significant decrease in the over-cured areas at the bottom part and especially on the middle empty area. Despite the 1 *mm* cavity on the first fabrication trial, a 6mm depth hole is created with the use of the algorithm and a major improvement on the dimensional accuracy is reached.

Another complex structure used for testing the capabilities of the iterative learning algorithm is given in Figure 3.14. For the top down fabrication strategy in stereolithography, stair-stepping effect and meniscus like shapes caused by the layer by layer projection is a common research subject.

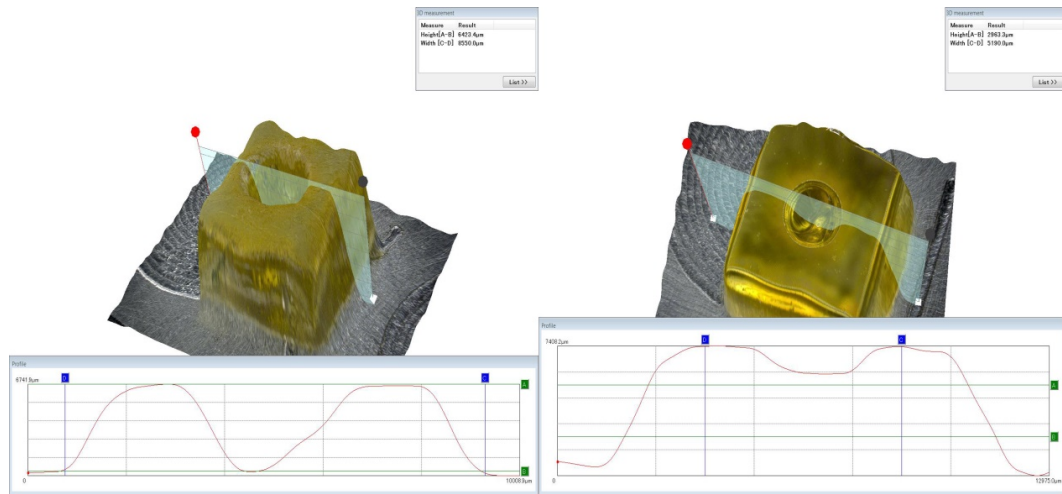


Figure 3.13: Measurement on the right side shows without the algorithm the depth of the hole is 1mm but using the algorithm depth reaches 6 mm.

Over-curing and light attenuation to the underlying layers are the reasons of irregularities in the fabrications. Structure used for this testing includes stair like levels and an empty part on the upper side to increase the difficulty for the fabrication. Developed algorithm is expected to decrease the effect of undesired attenuation up to a certain level within the limitations of the chemical process. Therefore, mentioned shape is expected to show the over-curing and better cavity area with the use of varying speed amounts in different layers.

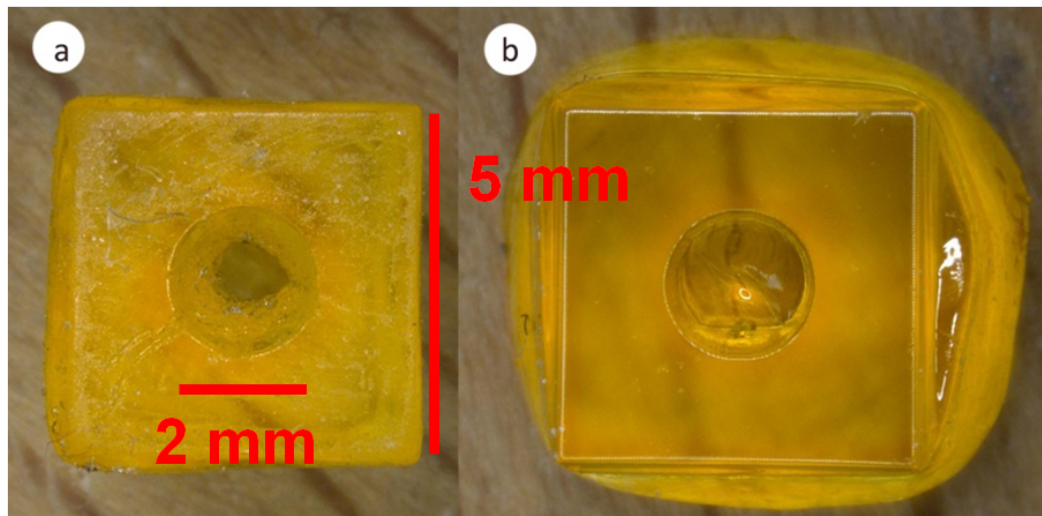


Figure 3.14: Over-cured areas disappear by using the algorithm (a), fabrication example with the starting parameter of the algorithm (b).

Firstly, to observe the nature of the process with the same speed usage throughout the whole fabrication, 4, 3 and 2 second fixed exposure times are used for measuring the over-cure amount and structural orientation. (Fig. 3.15)

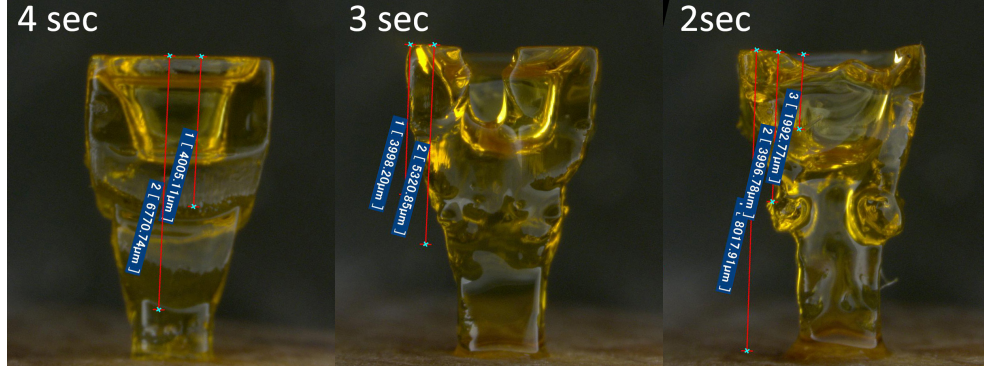


Figure 3.15: Fabrication trials with fixed exposure times of 4, 3 and 2 seconds and fabrication times of 40, 30 and 20 mins.

Measurements of these fabrications showed that 4 seconds fixed exposure resulted in high amount of over-curing but good formation of the cavity part on the upper side of the structure. 3 second fixed exposure time for all layers had better results in terms of over-curing but the structural integrity of the part is damaged both for the stairs side and the upper area. Lastly 2 second of exposure resulted in complete loss of structural layout even though pretty small amount of over cured areas could be observed but could not be measured. Results of these trials showed that with the use of a single parameter for the whole layers did not result in fabrication of desired shapes.

After the fabrication trials with single parameter usage in all layers, starting parameter of 4 seconds is applied on the algorithm. The initial iteration of the algorithm uses that parameter for all layers and measures the error amount at the end of the loop using the fabrication data calculated by the model. That error values for all layers are used to determine the change of fabrication parameters on the next iteration as explained in the iterative learning scheme. 4 iterations are done in the model to get the optimum parameters for the best fabrication possible. Then these values are applied on the system controllers and final fabrication is done on the device for comparing the error decrease of the model with the real life process.

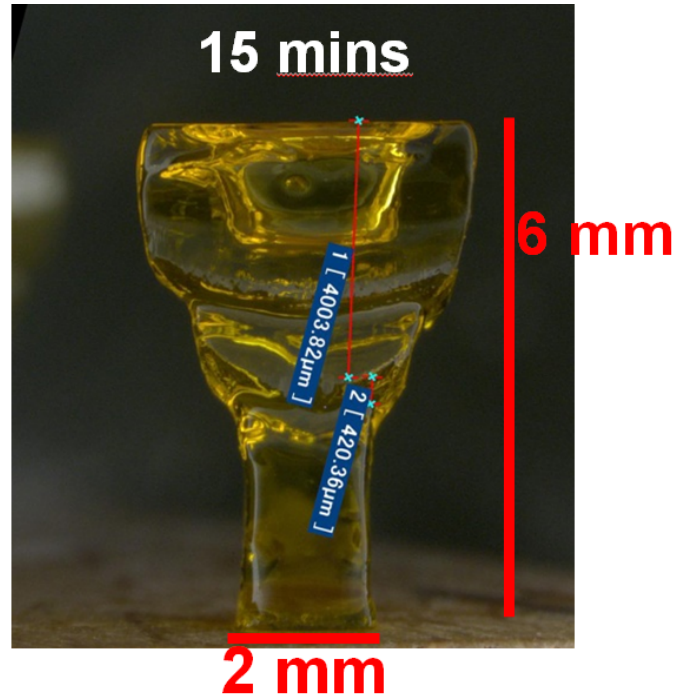


Figure 3.16: Fabrication of the complex shape using adjusted parameters found with the use of iterative learning scheme in a total fabrication time of 15 mins.

Fabrication of the complex shape on the system with the parameters adjusted by the algorithm, resulted in huge amount of error decrease. Over cure length measured as  $2700 \mu m$  with 4 seconds exposure interval is decreased to  $420 \mu m$ .(Fig. 3.16) Apart from that, adjusted fabrication speeds changed the total fabrication time of the part. With usage of 2 seconds total exposure time for a single layer, total fabrication time is measured as 20 minutes and structural integrity of the part was extremely low as most of the part was under-cured and it was impossible to measure the over-cured areas because of the lost integrity. Using the adjusted parameters, total fabrication took only 16 minutes and apart from the high regularity when compared to 2 seconds, over-cure length is decreased up to 85% when compared to initial 4 second fabrication of the iterative learning scheme.(Table 3.1)

The last shape used for showing the improvements is a gear structure. For showing the whole process steps, images of the CAD design, actual shape projected on the surface and desired layer shape is shown.(Fig. 3.17)

Table 3.1: Differences between varying single layer fabrication times

	2 sec	3 sec	4 sec	Algorithm
Fabrication Time	20 mins	30 mins	40 mins	16 mins
Over-Cure	Could not be observed	1320 $\mu m$	2700 $\mu m$	420 $\mu m$
Structural Integrity / Cavity	No/ Yes	Low/ Yes	High/ Yes	High/ Yes

6 teeth of the gear and empty part placed in the middle area defines the complexities of the structure. Heights of the fabricated parts are changed between 3 and 4 mm. Also in order to observe the possible differentiations on the final product, gears are produced with varying scales.

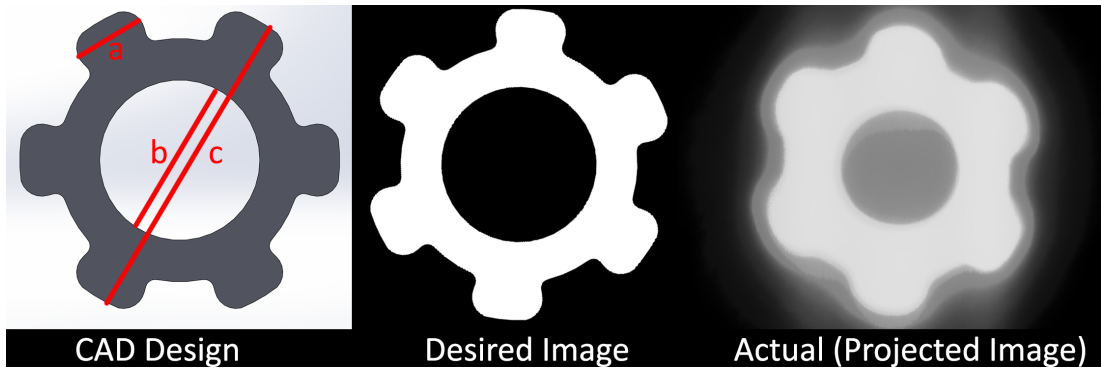


Figure 3.17: Design of the gear structure with actual and reference images.

Firstly for observing the changes on fabrications, parts are made with changing layer exposure time adjusting gains. Change of gains are observable in the error amounts of simulations but also it is expected to be observed using the real life application of the process. (Fig. 3.18)

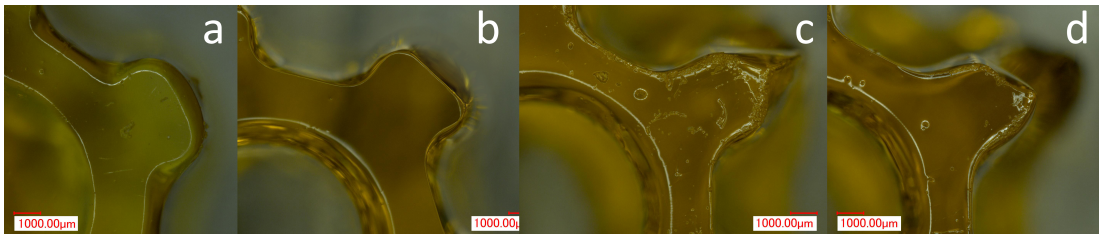


Figure 3.18: Picture a shows the fabrication without algorithm. Picture b, c and d is results of fabrications with the algorithm but changing amount of gains.

With the adjusted optimum gain of  $6 * 10^{-6}$ , fabrication results showed important amounts of improvements in the two previously defined areas of gear teeth and the empty part. (Fig. 3.19) Use of the single velocity parameter for all layers resulted in a nearly completely over-cured area in the middle part leaving only a less than  $500\mu m$  cavity.

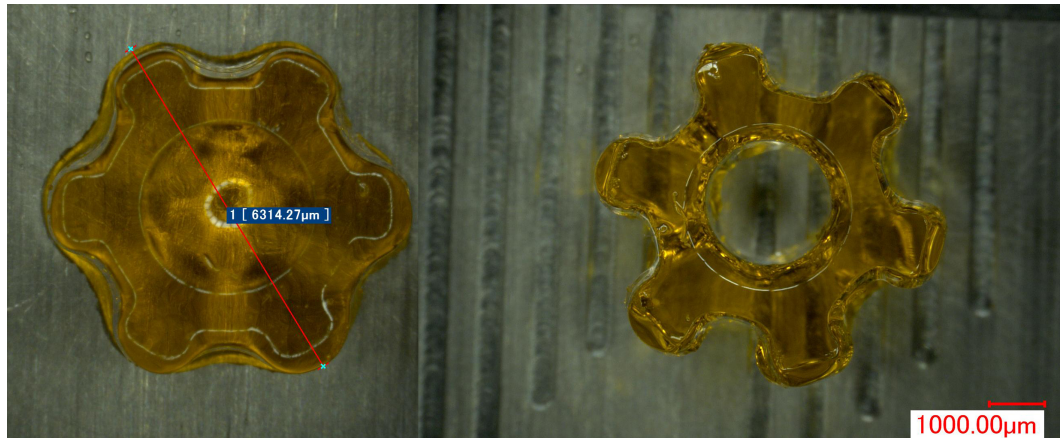


Figure 3.19: Fabrication without and with the use of the algorithm on scale x2.5.

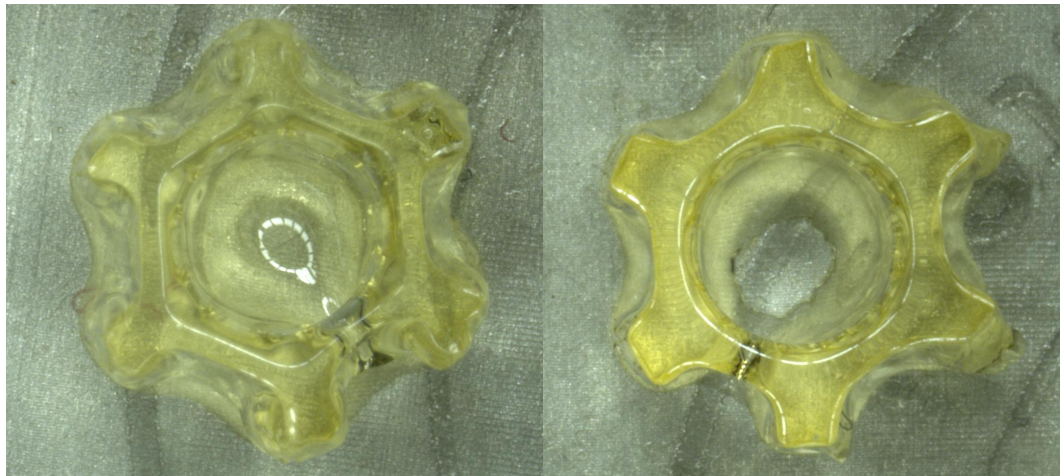


Figure 3.20: Fabrications with scale x2.

Lastly, in order to observe the effectiveness of the algorithm also in different dimensions, 3 fabrications with varying scales are made. Initial fabrication done before hand is done with x2.5 scale and 400 layers. New fabrications are with x2 and x1.5 scales with 300 and 200 layers respectively. When the dimensions are decreased in x2 scale, the results of the algorithm usage improved the fabrication quality.

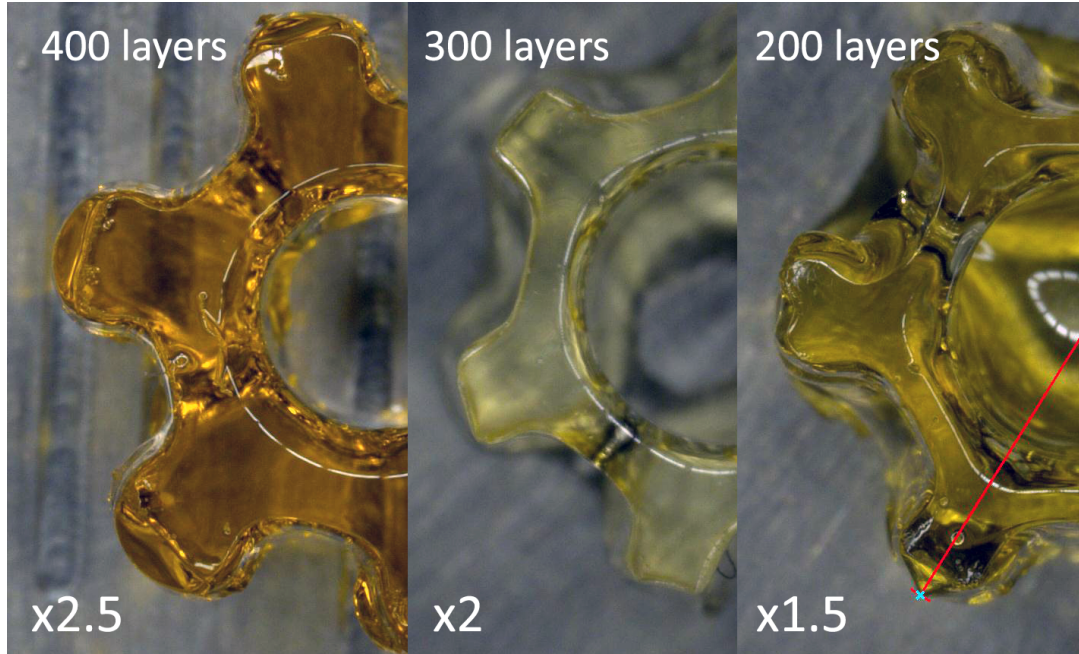


Figure 3.21: Fabrications with different dimensional scales.

But further decrease of dimensions especially down to 200 layers caused the reduction of the effectiveness. This is originated from the work”ing scheme of the algorithm which is based on the adjustment of layer parameters depending on the other layers. As the total error amount gets less, it causes smaller fluctuation in the parameters.(Fig. 3.21)

Table 3.2: Measured vs. actual dimensions in different scaled gear fabrications.

Area / Scale	2.5	Actual	2	Actual	1.5	Actual
a (Outer Over-Cure)	6.39	6	5.07	4.8	3.81	3.6
b (Inner Over-Cure)	2.8	3	1.12	2.4	0	1.8
c (Teeth Over-Cure)	2.65	2.2	1.43	1.76	1.71	1.32

Measured dimensions are given in (Table 3.2). Areas showing the measured dimensions are shown in (Fig. 3.17). These results shows that the decrease of layer number causes less changing in algorithms parameter adjustment amount. Therefore, smaller scaled fabrication of x1.5 resulted in huge over-cured areas especially in the inner area and gears.

### 3.3.4 Analysis of Results

Results of the validation trials demonstrated a remarkable amount of error decrease in the DLP based stereolithography process with the proposed iterative learning scheme for adjusting the process parameters. Materials, positioning system or the layer image projection are important subjects of this technique but also design of the part to be fabricated is important too. Therefore, apart from the aforementioned process parameter to be adjusted by the iterative learning algorithm, also shape of the fabricated parts is shown as a variable during the trials. Aim of the research was to develop an algorithm that is capable of decreasing the fabrication errors as much as possible even though the desired shapes vary.

For basic shapes, both simulations and validation trials showed similar amounts of developments in terms of decreasing the over or under-cured areas similar as the total fabrication errors experienced during the process. Up to 80% decrease is reached in the simulations and nearly 75% error decrease is observed in the fabrications.

Complex forms showed distinct results when compared to the basic shapes. There are couple of reasons for that differentiation which could be discussed. Simulations based on the iterative learning algorithm showed nearly 40% decrease in total error amount for the complex shape. But in the validation fabrications, this improvement amount increased more than 75%. Application of the algorithm to device resulted with unexpectedly high amount of improvement in fabrication quality when compared to the simulated errors according to the model.

#### 3.3.4.1 Shape Variance

Firstly, modelling of the system could be given as the main reason of variances between the simulations made according to the model and real life fabrication trials. Lots of process parameters about the material, optical system, projector and positioning system are included in the model. Some of them are found through

experiments and measurements but some are taken directly from the data sheets of the parts. All of the possible errors emerging from tens of measurements could be affecting the whole process model. Also the modelling of the complete chemical process is an extremely complicated process as the solidification starts from the structural changes and differentiations occurring on the small molecules and building blocks of the polymer resin which is not directly included in the model but used with the adoption of already existing cure models based on different physical laws.

Secondly, learning algorithm might be causing the differences in different shapes. Algorithm was not created to evaluate the shapes and act according to that. When the step like structures is examined, it could be observed that the resultant amount of over-cured areas increases especially under the overlying stairs.

Algorithm acts and tries to overcome this stair stepping effect by decreasing the exposure amounts of layers above directly. As the algorithm changes the exposure directly proportional to the error amount of the layer, for the over-cured areas under the stair like shapes, it decreases the exposure amounts in an increased rate because of the high number of wrongly cured pixels located on that specific layer. (*Fig. 3.22*) Similarly for differently designed structures, algorithm can cause unexpected improvements but also it can result in increase of the error amounts too. From the validation experiments and simulation results, no negative effect on the error decreasing is observed with the developed algorithm. It always acted in the direction of changing the exposure amounts in all layers towards less curing errors.

Lastly, shape differences could be correlated with a new area of research named as the design for 3d printing. Materials, systems capabilities and also application of the selected additive manufacturing technique create limitations on the effective usage of 3d printing systems. It can limit the fabrication process in terms of dimensions like feature size, shape details like cavities or holes, structural properties like roughness or hardness and lots of other fabricated part properties.

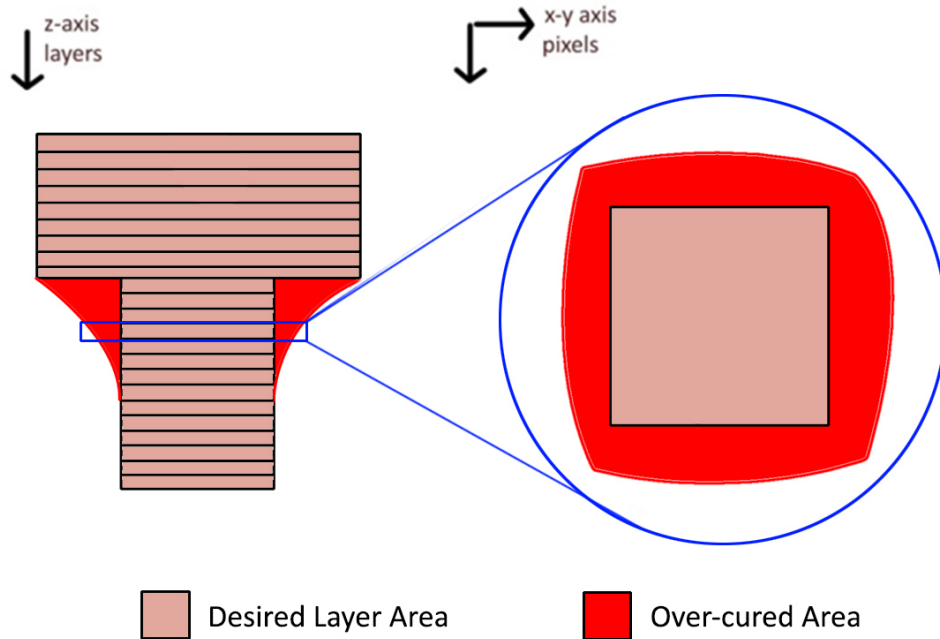


Figure 3.22: Image showing the high amount of over-curing under the stair shape.

Therefore, according to the established system, various design constraints can be determined and listed like an instruction manual. Especially about the shapes, possible depth of the cavities and holes or heights and widths of the indented parts like stair shaped structures that are producible could be listed. While the trials are made for validating the algorithm, effects of the stair like shapes could be observed easily. With the use of the algorithm, as fabrication results could be estimated, design restrictions and limitations could be noted with further work.

Previous examples of fabricating the stair like stepped structures showed that direction of manufacturing is also an important aspect of design and solidification for stereolithography. These type of structures can be placed downwards and upwards on the fabrication platform which creates important amount of variance in the resultant part quality.(Fig. 3.23) Developed algorithm showed significant improvement for the case of upside-down fabrication. Reason of the need for enhancement in reverse fabrication arises from the need of development in stereolithography process, independent of limitations that design for additive manufacturing causes.

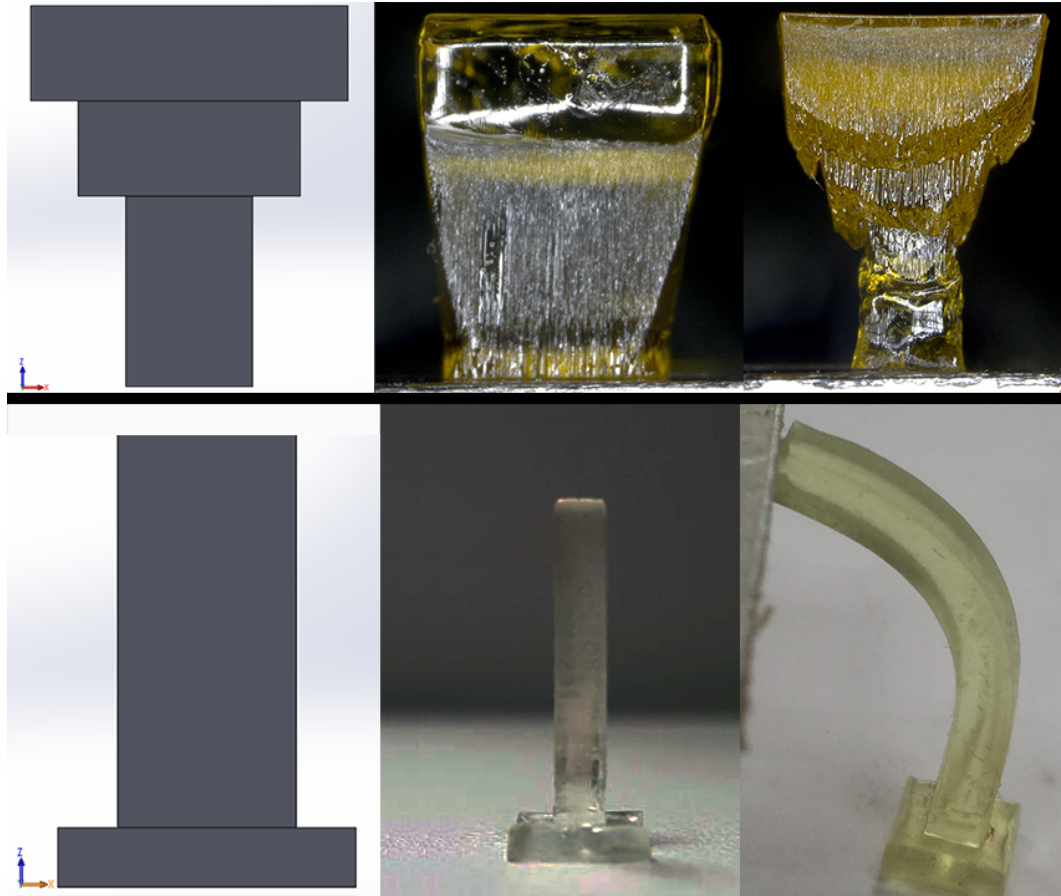


Figure 3.23: Upside-down and straight positioned fabrications of stair like structures without the algorithm.

### 3.3.4.2 Fabrication Time

Another extremely important result observed with the use of the iterative learning algorithm is the change of the fabrication time. Nature of the algorithm adjusts the speed of the fabrication platform for every layer interval of the process. This is directly proportional with the exposure time interval of that layer so the summation of all layers intervals results in the total process time. Without the use of the algorithm, total fabrication times were direct multiplication of the layer number and the layer exposure time interval.

Optimized parameters found through experimental work about the parameter optimization for fabrication of high aspect ratio structures mentioned in chapter

1.3, are used in the early validation trials done without the algorithm. As described in section 3.3, structure of a single parameter fabrication that takes 20 minutes defines the lower edge of the structural integrity and another fabrication of 40 minutes provides a better layout with high over curing.

Measurements showed going beyond these values will result in a huge divergence in the amount of curing errors for all layers. Use of the algorithm and defining changing amount of speeds to all layers, resulted in a 16 minute fabrication having better properties in all aspects when compared to the initials. So, apart from decreasing the error of fabrication, algorithm acted as an optimization scheme in another way and decreased the total fabrication time significantly, which is an extremely valuable output for a manufacturing system.

# Chapter 4

## Conclusion and Future Work

The work presented in this M.S. thesis covers the development of an iterative learning control algorithm for increasing the fabrication quality of a DLP projection based micro stereolithography system. Developed parameter control scheme is used to adjust the critical process parameter with iterations for decreasing the error amounts of the fabrication process determined according to the problem definition. Subsequently, properties of the established manufacturing system are investigated based on its all components. These components include the positioning system, optical system, control software and as one of the most important parts of an additive manufacturing system the chemical resin.

Initial experiments with the system included fabrication of different structures like high aspect ratio shapes, micro needles, sensor components, scaled buildings etc. These examples emerged some questions about the chemical process, how the solidification occurs and how the process could be defined mathematically. Based on the literature search defining existing laws and mathematical explanations, measurements and experiments are made to obtain the system parameters expressing the working scheme of all components. These included resin specifications like critical energy, depth of penetration and layer image projection measurements like irradiation and light distribution on the fabrication surface.

Finding all of the parameters made it possible to replicate the fabrication process mathematically by creating a simulation code based on the calculation of the curing amount for all pixels on each layer. This calculation defines whether a point defined as a pixel is solidified or not at the end of light exposure of all layers when the process ends. Comparing this information with the knowledge of how the desired 3d shape should be cured at the end, makes an error calculation possible defined on layers.

This information about the incorrectly cured pixel areas is then used in the correction algorithm. Based on the most significant property of the system, which is the continuous movement of fabrication platform on z-axis, parameter most importantly affecting the fabrication process and exposure is decided as the platform speed. Highly capable positioning device available as a component of the system supported the decision to choose this parameter for adjusting the process output.

Then for adjusting the parameter, an iterative learning control scheme is created to adjust the parameter in iterations according to the error amounts found by the fabrication simulation. Advanced and final algorithm developed, changes the platform speeds of layers by multiplying a learning gain with the layers error value input. Therefore, a new speed command is created to decrease the error amount on the next iteration.

For changing a specific layers parameter, not only the error amount on that one but the errors of the underlying or overlying layers are also taken into consideration. Reason for this calculation is the attenuating nature of the light inside the liquid resin used for the fabrication. When the process is going on and exposure is applied on a specific layer, light attenuating inside also effects the solidification of other layers. This results in errors named as over and under-curing of the fabricated areas. Accordingly, presented algorithm change the parameter based on the character of the chemical solidification process.

Decreasing the number of fabrication trials which results in excessive usage of resin and time, only simulations are used to observe and guess the algorithm

results for reaching best quality fabrications having minimum amount of error. Based on the fabricated shapes properties, up to 80% decreasing trend in the error amounts are observed with the measurements. Furthermore, an impressive decrease in the total fabrication time of these parts is reached with the use of the designed iterative learning controller.

Experimental results of this research show significant improvements with the use of the developed algorithm. However, variances between the simulation results and validating fabrication trials show that the mathematical modeling of the curing process could be improved in many ways. All experiments and measurements done to find out the process parameters could be renewed to be done in a more detailed way. Many scientific areas like physics, chemistry and optics are included in these experimental studies so detailed work on all of them should be done to improve the accuracy of the algorithm.

Optical system of a stereolithography system especially with a DLP projector light source is an important component as it should diverge and reflect the light on the fabrication surface correctly. A more complicated optical system with advanced components could be used and the reflection process could be included in the process model. It would increase the precision of the layer image and increase the fabrication quality by projecting sharper details on the surface.

Chemical resin polymer used as the raw material is another important topic. Structure of the material could create limitations in the minimum detail size of the fabrication and also could affect the solidification process in terms of needed time and energy. So the resin could be examined and regenerated in order to reach the desired fabrication goals.

Lastly, apart from the properties and modeling of the system, iterative learning scheme can be improved to be more efficient and effective to control the process parameter. Loop numbers could be decreased by rearrangement of the process, as algorithm makes huge numbers of calculations for finding exposures on each pixel of all layer with the effect of attenuation.

Another important issue is the observation of the fabrication while the system is working. On-line measurement of the light intensity and feeding of data to the learning algorithm could improve the control scheme and provide instant or faster correction. But on-line imaging of the fabrication area is an important amount of work as the exposure area is placed under liquid resin. A second parameter such as light intensity, which is controlled from the light source, could be added to the adjusting algorithm in order to further reduce the error.

# Bibliography

- [1] E. O. Olakanmia, R. F. Cochranea, K. W. Dalgarno, “A review on selective laser sintering/melting (SLS/SLM) of aluminium alloy powders: Processing, microstructure, and properties,” *Progress in Materials Science* , vol. 74, pp. 401 - 477, 2015.
- [2] W. Zhang, L. Han and S. Chen, “Integrated Two-Photon Polymerization With Nanoimprinting for Direct Digital Nanomanufacturing,” *Journal of Manufacturing Science and Engineering* , vol. 132, no. 3, 030907, 2010.
- [3] M. Hatzenbichler, M. Geppert, S. Gruber, E. Ipp, R. Almedal, and J. Stampfl, “DLP-based Light Engines for Additive Manufacturing of Ceramic Parts,” *Emerging Digital Micromirror Device Based Systems and Applications*, vol. 4, 2012.
- [4] J. Choi, R. B. Wicker, S. Cho, C.S. Ha and S.H. Lee, “Cure Depth Control for Complex 3D Microstructure Fabrication in Dynamic Mask Projection Microstereolithography,” *Rapid Prototyping Journal*, vol. 15, no. 1, pp. 59 - 70, 2009.
- [5] M. Hatzenbichler, M. Geppert, R. Seemann and J. Stampfl, “Additive Manufacturing of Photopolymers Using the Texas Instruments DLP Lightcrafter,” *Emerging Digital Micromirror Device Based Systems and Applications*, vol. 5, 2013.
- [6] J. H. Lee, R. K. Prud’homme and I. Aksay, “Cure Depth in Photopolymerization: Experiments and Theory,” *Journal of Materials Research*, vol. 16, no. 12, pp. 3536 - 544, 2001.

- [7] S. H. Chiu, S. H. Pong, D. C. Wu and C. H. Lin “A Study of Photomask Correction Method in Areaforming Rapid Prototyping System,” *Rapid Prototyping Journal* , vol. 14, no. 5, pp. 285 - 92, 2008.
- [8] U. Berger and B. Maule, “Rapid Manufacturing of High Reduction Polymer Gears by Use of Stereolithography,” *2009 IEEE/ASME International Conference on Advanced Intelligent Mechatronics*, 2009.
- [9] A. K. Au, W. Lee and A. Folch “Mail-order Microfluidics: Evaluation of Stereolithography for the Production of Microfluidic Devices,” *Lab Chip*, vol. 14, no. 7, pp. 1294 - 301, 2014.
- [10] R. Gauvin, Y. C. Chen, J. W. Lee , P. Soman, P. Zorlutuna, J. W. Nichol, H. Bae, S. Chen and A. Khademhosseini “Microfabrication of Complex Porous Tissue Engineering Scaffolds Using 3D Projection Stereolithography,” *Biomaterials*, vol. 33, no. 15, pp. 3824 - 834, 2012.
- [11] W. Meyer, S. Engelhardt, E. Novosel, B. Elling, M. Wegener and H. Krger, “Soft Polymers for Building up Small and Smallest Blood Supplying Systems by Stereolithography,” *Journal of Functional Biomaterials*, vol. 3, no. 4, pp. 257 - 68, 2012.
- [12] J. P. Partanen, “Enhanced Resolution of Stereolithography,” *Proceedings of European Meeting on Lasers and Electro-Optics CLEOE-96* , 1996.
- [13] C. Sun, N. Fang, D.M. Wu and X. Zhang, “Projection Microstereolithography Using Digital Micro-mirror Dynamic Mask,” *Sensors and Actuators A: Physical*, vol. 121, no. 1, pp. 113 - 20, 2005.
- [14] G. W. Hadipoespito, Y. Yang, H. Choi, G. Ning and X. Li, “Digital Micromirror Device Based Microstereolithography for Micro Structures of Transparent Photopolymer and Nanocomposites,” *Solid Freeform Fabrication Proceedings 14th, Solid Freeform Fabrication Symposium; 2003; Austin, TX*, pp. 13 - 24, 2003.
- [15] A. Ovsianikov, S. Schlie, A. Ngezahayo, A. Haverich and B. N. Chichkov,

- “Two-photon Polymerization Technique for Microfabrication of CAD-designed 3D Scaffolds from Commercially Available Photosensitive Materials,” *J Tissue Eng Regen Med Journal of Tissue Engineering and Regenerative Medicine*, vol. 1, no. 6, pp. 443 - 49, 2007.
- [16] D. Lee, T. Miyoshi, Y. Takaya and T. Ha, “3D Microfabrication of Photosensitive Resin Reinforced with Ceramic Nanoparticles Using LCD Microstereolithography,” *JLMN-Journal of Laser Micro/Nanoengineering*, vol. 1, no. 2, pp. 142 - 48, 2006.
- [17] J. Stampfl, S. Baudis, C. Heller, R. Liska, A. Neumeister, R. Kling, A. Ostendorf, and M. Spitzbart, “Photopolymers with Tunable Mechanical Properties Processed by Laser-based High-resolution Stereolithography,” , vol. 18, no. 12, 125014, 2008.
- [18] A. Yebi and B. Ayalew, “Optimal Layering Time Control for Stepped-Concurrent Radiative Curing Process,” *Journal of Manufacturing Science and Engineering* , vol. 137, no. 1, 011020, 2014.
- [19] A. S.Jariwala, F. Ding, X. Zhao and D. W. Rosen, “A Process Planning Method for Thin Film Mask Projection Micro-Stereolithography,” *29th Computers and Information in Engineering Conference, Parts A and B*, vol. 2, 2009.
- [20] X. Zhao, “PROCESS PLANNING FOR THICK-FILM MASK PROJECTION MICRO STEREO LITHOGRAPHY,” Master’s thesis, Georgia Institute of Technology, May 2009.
- [21] A. Yebi and B. Ayalew, “Partial Differential Equation-Based Process Control for Ultraviolet Curing of Thick Film Resins,” *Journal of Dynamic Systems, Measurement, and Control* , vol. 137, no. 10, 101010, 2015.
- [22] X. Zhao and D. W. Rosen, “Process Modeling and Advanced Control Methods for Exposure Controlled Projection Lithography,” *Proceedings of American Control Conference 2015*, pp. 3643 - 3648, 2015.

- [23] A. S. Jariwala , R. E. Schwerzel, M. Werve and D. W. Rosen, “Two-Dimensional Real-Time Interferometric Monitoring System for Exposure Controlled Projection Lithography,” *ASME/ISCIE 2012 International Symposium on Flexible Automation*, 2012.
- [24] A. S. Jariwala , R. E. Schwerzel and D. W. Rosen, “Real-Time Interferometric Monitoring System for Exposure Controlled Projection Lithography,” *Proc. of Solid Freeform Fabrication Symposium*, pp. 99 - 110, 2011.
- [25] A. Yebi, B. Ayalew and S. Dey “Observer Design for State Estimation of UV Curing Processes,” *Volume 2: Dynamic Modeling and Diagnostics in Biomedical Systems; Dynamics and Control of Wind Energy Systems; Vehicle Energy Management Optimization; Energy Storage, Optimization; Transportation and Grid Applications; Estimation and Identification Methods, Tracking, Detection, Alternative Propulsion Systems; Ground and Space Vehicle Dynamics; Intelligent Transportation Systems and Control; Energy Harvesting; Modeling and Control for Thermo-Fluid Applications, IC Engines, Manufacturing* , 2014.
- [26] J. Potgieter, J. R. Zyzalo, O. Diegel and W.l. Xu. , “Layer Curing for Masked Projection Stereolithography: The Effects of Varying Irradiance Distributions,” *2008 15th International Conference on Mechatronics and Machine Vision in Practice* , 2008.
- [27] Y. Pan, X. Zhao, C. Zhou and Y. Chen, “Smooth Surface Fabrication in Mask Projection Based Stereolithography,” *Journal of Manufacturing Processes* , vol. 14, no. 4, pp. 460 - 70, 2012.
- [28] Z. Ali, “Process modelling for projection based stereo lithography,” Master’s thesis, Bilkent University, Ankara, August 2015.
- [29] P. F. Jacobs, “Stereolithography and Other RP&M Technologies: From Rapid Prototyping to Rapid Tooling,” *ASME*, New York, 1996.
- [30] A. S. Limaye, D. W. Rosen “Process Planning Method for Mask Projection Microstereolithography,” *Rapid Prototyping Journal* , vol. 13, no. 2, pp. 76 - 84, 2007.

# Appendix A

## Matlab Code

This section includes the Matlab codes defining the various processes for the iterative learning algorithm. Image processing, model simulations based on the mathematical model and pixel cure model, error amount calculation and iterative parameter learning scheme are listed below.

### A.1 Image Processing

```
RGB = imread('holl.jpg'); %Projected Shape
I = rgb2gray(RGB); % Uncalibrated Irradiance, Pixel values
averagelight = mean2(I);
[d1,d2,d3] = size(RGB);

RGB2 = imread('holla.jpg'); %Desired Shape
I2 = rgb2gray(RGB2);
I2 = double(I2);
averagelight2 = mean2(I2);
[d4,d5,d6] = size(RGB2);
p2 = ae2/averagelight2;
ex2 = p2.*I2;
ex2 = double(ex2);
```

## A.2 Actual Model Simulation

```
content.    for actuallayer = 1:lmax;

timetot = timetot + sec(actuallayer);
k = (1-(0.2406*exp(timetot)-0.3491));
ae = 6.21*sec(actuallayer); % Uncalibrated average exposure
p = ae/averagelight; % Exposure calibration
ex = p.*I; % Calculates exposure for all points in a single layer
ex = double(ex);

for j = 1:d1;
for h = 1 :d2;
if actuallayer ==1
ie = ex(j,h);
b = ie;
final(j,h) = b; % Exposure of all points in top layer
end
if actuallayer > 1
ie = ex(j,h);
final(j,h)=final(j,h)+ie*exp(-x*actuallayer/d); % Exposure of all
%points in other layers
end
end
end

p=0;
for j = 1:d1;
for h = 1:d2;
p = final(j,h);
if p >= critE; % If Exposure is larger than Critical E,
%puts a dot on that point.
final2(j,h) = drawpixel;
else
final2(j,h) = 0; % Otherwise, leaves that space empty
end
end
end
```

### A.3 Reference Model Simulation

```
p2=0;

for j = 1:d1;
for h = 1:d2;
p2 = I2(j,h);
if p2 > 5;
finalo2(j,h) = drawpixel;
else
finalo2(j,h) = 0;
end
end
end
```

### A.4 Error Calculation

```
err = 0;

for j = 1:d1;
for h = 1:d2;

if final2(j,h) == finalo2(j,h);
err = err;
elseif final2(j,h) < finalo2(j,h);
err = err + 1;
elseif final2(j,h) > finalo2(j,h);
err = err - 1;
end

end

end

error(actuallayer) = err;
```

## A.5 3D Simulation Result

```
drawpixel = drawpixel-1;
shading interp
surf(final2) % Simulation Result
```

## A.6 Parameter Control Algorithm

```
coef2 = 8*10(-5);
for i = 1:lmax;
interv = 10; % +/- layer number to count in average error calculation
chnng = 350;
si=0;
sym=0;
si2=0;
sym2=0;
if i < lmax - interv + 1 && i > interv;
if error(i) < 0;
for si = i:(i+interv-1);
sym = sym+error(si);
end
sec(i) = sec (i) + coef*(sym/interv);
for count = 1:chnng;
if i-count>0;
sec(i-count) = sec(i-count)+coef2*(sym/interv)*(1/(i-count)2);
else
end
end
elseif error(i) > 0 %&& u<5;
for si2 = (i-interv+1):i;
sym2 = sym2+error(si2);
end
sec(i) = sec (i) + coef*(sym2/interv);
for count = 1:chnng;
if i-count>0;
```

```

sec(i-count) = sec(i-count)+coef2*(sym/inter)* (1/(i-count)^2);
else
end
end
else
sec(i) = sec(i);
end
else
if error(i) < 0 ;
for si = i:lmax;
sym = sym+error(si);
end
sec(i) = sec (i) + coef*(sym/(lmax-i+1));
for count = 1:chn;
if i-count>0;
sec(i-count) = sec(i-count)+coef2*(sym/inter)* (1/(i-count)^2);
else
end
end
elseif error(i) > 0 %&& u<5;
for si2 = 1:i;
sym2 = sym2+error(si2);
end
sec(i) = sec (i) + coef*(sym2/i);
for count = 1:chn;
if i-count>0;
sec(i-count) = sec(i-count)+coef2*(sym/inter)* (1/(i-count)^2);
else
end
end
else
sec(i) = sec(i);
end
end
for fi=1:lmax
if sec(fi) <= 0.01
sec(fi) = 0.01;
end
end
end

```

# Appendix B

## Nomenclature

$A$	Absorbance
$\epsilon$	Attenuation coefficient
$E_c$	Critical Exposure
CAD	Computer aided design
$c$	Concentration
$C_d$	Cure depth
$Err$	Cure error, number of wrongly solidified pixels
$d$	Defined layer interval
$z$	Depth, length in z-direction
$D_p$	Depth of penetration
DLP	Digital light processing
DMD	Digital micromirror device
$E$	Exposure
$E_z$	Exposure at a specific depth $z$
$I$	Irradiation
$\mu m$	Micrometer
$\epsilon$	Molar absorptivity
$nm$	Nanometer
$LT$	Layer thickness
$l$	Length, layer thickness
3D	Three dimensional
$T$	Transmittance
UV	Ultraviolet
$\lambda$	Wavelength